

Cost Effective Optimised Synthetic Surface Modification Strategies for Enhanced Control of Neuronal Cell Differentiation and Supporting Neuronal and Schwann cell Viability

Caroline S. Taylor^{1*}, Rui Chen², Raechelle D' Sa², John A. Hunt³, Judith M. Curran²
and John W. Haycock^{1*}

¹ Department of Materials Science and Engineering, University of Sheffield, Sheffield,
S3 7HQ. U.K

² Department of Mechanical, Materials and Aerospace, University of Liverpool,
Liverpool, U.K.

³ Medical Technologies and Advanced Materials, Nottingham Trent University,
Nottingham NG11 8NS, U.K.

***CORRESPONDING AUTHORS**

Professor John W. Haycock
Department of Materials Science and Engineering
University of Sheffield
Sheffield
S3 7HQ.
U.K.

Email: j.w.haycock@sheffield.ac.uk

Telephone: +44 (0)114 2225972

Dr Caroline S. Taylor
Department of Materials Science and Engineering
University of Sheffield
Sheffield
S3 7HQ.
U.K.

Email: c.s.taylor@sheffield.ac.uk

ABSTRACT

Enriching a biomaterial surface with specific chemical groups has previously been considered for producing surfaces that influence cell response. Silane layer deposition has previously been shown to control mesenchymal stem cell adhesion and differentiation. However, it has not been used to investigate neuronal or Schwann cell responses *in vitro* to date. We report on the deposition of aminosilane groups for peripheral neurons and Schwann cells studying two chain lengths: 1) 3-aminopropyl triethoxysilane (short chain-SC) and 2) 11-aminoundecyltriethoxysilane (long chain-LC) by coating glass substrates. Surfaces were characterised by water contact angle, AFM and XPS. LC-NH₂ was produced reproducibly as a homogenous surface with controlled nanotopography. Primary neuron and NG108-15 neuronal cell differentiation and primary Schwann cell responses were investigated *in vitro* by S100 β , p75 and GFAP antigen expression. Both amine silane surface supported neuronal and Schwann cell growth, however neuronal differentiation was greater on LC aminosilanes versus SC. Thus, we report that silane surfaces with an optimal chain length may have potential in peripheral nerve repair for the modification and improvement of nerve guidance devices.

KEY WORDS: Peripheral nerve injury; dorsal root ganglion; surface chemistry; amine; silane; surface coating

1 INTRODUCTION

Peripheral nerve injuries affect 7 million people globally every year, and most commonly arise from trauma incidents ¹. Peripheral nerve has the ability to regenerate after injury by a process known as Wallerian degeneration and regeneration ². However, severity of injury determines the success of repair, and surgical intervention usually required ¹. An autograft or synthetic hollow nerve guide

conduit (NGCs) can be used to 'bridge' gaps between the ends of nerve stumps³. Nerve guide conduits are entubulation devices manufactured from both natural and synthetic materials¹, with an emerging number of FDA approved devices comprising hollow tubes, wraps and cuffs. However, nerve guide use is limited to short gap injuries (<20mm) and therefore autograft use is required for large gap injuries, >20mm. Though the current 'gold standard' treatment, autografts are associated with donor site morbidity and there is a lack of donor nerve available². This is focussing attention to NGC designs and methods for improvement, including surface topography and guidance cues for regenerating axons present in autografts³. Approaches used to improve hollow NGCs include the addition of intraluminal guidance scaffolds, incorporating channels and pores, coatings, and changing surface chemistry and topography.

The use of coatings have been shown to improve initial cellular adhesion with synthetic biomaterial surfaces e.g. extra cellular matrix (ECM) proteins¹. ECM coatings mimic native extracellular matrix cues and to an extent surface topography, providing the correct biochemical interactions for adhesion and potentially improving regenerative outcomes of a conduit³. Proteins such as laminin, collagen and fibronectin improve neuronal and Schwann cell adhesion and differentiation when incorporated into bioengineered NGCs¹. For device translation, the use of naturally-derived proteins must consider cost, potential batch variation, and unwanted immune response. Alternatively, synthetic coatings are scalable, reproducible and cost-effective⁴.

Synthetic coatings can control the type, level and conformation of serum proteins that adsorb¹. Alteration of the surface chemistry can influence protein surface conformation, and influence initial adhesion, proliferation and cell

differentiation⁵. Techniques such as plasma polymerisation have been used to alter biomaterial surface chemistry, without altering bulk material properties¹. Plasma deposition studies report on acrylic acid and allyamine surface modification improving SH-SY5Y neuronal cell adhesion and differentiation⁶ and air plasma techniques also increasing primary Schwann cell adhesion onto modified surfaces, increasing nerve regenerative properties of conduits when grafted with peptide or growth factors⁷. However, plasma polymerisation requires a high vacuum, limiting scale-up⁸, supporting a need for simpler surface modification.

Silane modification is a simple, cost effective, controllable and scalable technique for biomaterial modification. Previous work has demonstrated enrichment of surfaces with chemical reactive groups including amines, hydroxyl and carboxyl⁵. Silane modification can mimic the ECM by changing surface nano-topography, and substrate chemistry, providing a biological surface to enhance initial cell attachment and maintain proliferation⁹. Silane chain length has been shown to influence deposition of the chemical reactive group at submicron scale, and influence cell adhesion and differentiation due to topographic profile⁹.

We have previously reported that 11-aminoundecyltriethoxysilane surfaces supported osteogenic differentiation of mesenchymal stem cells, in contrast to 3-aminopropyl triethoxysilane¹⁰. Aminosilanes, of varying chain lengths, were fully characterised, using water contact angle, X-ray photoelectron spectroscopy and atomic force microscopy, to determine the effect of silane chain length on surface chemistry and topography at sub micron level. 11-aminoundecyltriethoxysilane modified surfaces presented an ordered nanoroughness, resulting in favourable 'surface chemistry and topography' for osteoinduction, but has not been investigated for other tissue engineering applications¹⁰.

In the context of nerve repair, one study has reported modifying chitosan using 3-aminopropyl triethoxysilane which promoted increased Schwann cell adhesion and proliferation¹¹. However, silane chain length has not been investigated thoroughly for nerve implant biomaterials. The aim of the present study was to investigate the influence of two different silane chain lengths, with known surface chemistry and topography, characterised from our previous study¹⁰, on neuronal and Schwann cell differentiation and phenotype.

2 MATERIALS AND METHODS

2.1 Preparation and modification of borosilicate glass coverslips - Glass

coverslips (13mm²) were modified with 3% aminosilanes (SC: 3-aminopropyl triethoxysilane; LC: 11-aminoundecyltriethoxysilane) as previously described¹⁰.

Briefly, glass coverslips were cleaned using a 0.5M solution of sodium hydroxide and then 1M Nitric acid for 30 minutes in an ultrasonic bath, followed by washing in three changes of distilled water, and dried in a 50°C oven. Clean coverslips were then modified using the 0.1M silanes, 3-Aminopropyl triethoxysilane (Sigma), and 11-Aminoundecyltriethoxysilane (Fluorochem), in pure isopropanol for 30 minutes. Samples were then rinsed with isopropanol and distilled water. All glass coverslips were sterilised with 70% ethanol for 30 minutes, and washed overnight with PBS before cell culture studies. Prior to cell seeding, 2µg/mL of fibronectin (Merck), in sterile PBS, was added to clean plain glass coverslips, as the control, and incubated at 37°C in 5% CO₂ for 30 minutes.

2.2 Water contact angle measurement - Dynamic contact angles of the samples in deionised purified water were measured using a Dynamic Contact Angle

Tensiometer (CDCA 100, Camtel Ltd., Royston, Herts, UK) at 22 ± 0.5 °C. Briefly, two samples were tightly stuck together on the unmodified side. Each sample was immersed into the wetting solution (deionised pure water) at a rate of 0.060 mm/s. The wetting force at the solid/liquid/vapour interface was recorded by an electrobalance as a function of time and immersion depth and was converted into an advancing contact angle. The values reported for dynamic advancing angles of modified glass coverslips are mean and standard deviations of $n = 4$.

2.3 X-ray photoelectron spectroscopy (XPS) – Elemental surface chemistry, of aminosilane modified substrates, was confirmed using XPS as previously described¹⁰.

2.4 Atomic force microscopy (AFM) - Atomic force microscopy was used to confirm surface topography, previously reported, of the NH₂ modified substrates. AFM was performed as previously described¹⁰. Mechanical properties of silane glass surfaces were investigated by fitting the AFM data obtained with the Derjaguin–Muller–Toporov (DMT) model to extract the elastic modulus of modified glass substrates by fitting the contact region of the retract curve close to the contact point.

2.5 NG108-15 cell culture – An NG108-15 (ECACC 88112303) cell line was used for study. They were originally created from Sendai virus mediated fusion of a mouse neuroblastoma and rat glioma cells. They are a valuable experimental *in vitro* tool for quantifying neurite development as a proxy for primary neuronal cell differentiation. Herein they will be referred to as NG108-15 neuronal cells in this context¹², with experimental culture and conditions used for experiments as

previously described ¹². Cultures were maintained for 6 days, changing the culture medium to serum free Dulbecco's Modified Eagle Medium (DMEM) after 2 days in culture.

2.6 Isolation and culture of primary Schwann cells – Rat primary Schwann cells were isolated and cultured as previously described ¹³. Schwann cells were cultured up to passage 7 for experiments. 60,000 Schwann cells, per sample, were seeded onto surfaces for 6 days and medium replaced once at day 3.

2.7 Isolation and dissociation of dorsal root ganglion bodies (DRGs) -

Dissociation of DRGs into co-cultures of primary neurons and Schwann cells was performed using the methods as previously described ¹⁴. Co-cultures were maintained in F12 medium (containing 2 mM glutamine, 1% penicillin/streptomycin and 0.25% amphotericin B) supplemented with the addition of 100ug/mL bovine serum albumin (BSA), 10 μ L/mL of N₂ and 77ng/mL of nerve growth factor (NGF). Cells were left in culture for 7 days, and medium changed at day 4.

2.8 Live/dead analysis of NG108-15 cells and primary Schwann cells -

Cell viability was confirmed by live/dead analysis, and samples imaged using confocal microscopy as previously described ¹². Cells were counted using a ITCN cell counter plugin on Image J NIH software ^{15, 16}.

2.9 Immunolabelling of NG108-15 cells, Schwann cells and dissociated dorsal

root ganglia – Modified coverslips containing NG108-15 cells only, Schwann cells only, and those containing dissociated DRG cultures, were labelled for cell type specific antigens, and imaged using confocal microscopy as previously described ¹². NG108-15 cells and primary neurons were labelled for β III-tubulin (neurite marker)

and Schwann cells labelled for S100 β in co-culture with primary neurons. Mono-culture of primary Schwann cells on modified substrates were labelled for S100 β , Glial fibrillary acidic protein (GFAP) low-affinity nerve growth factor receptor (p75NGFR) as previously described ¹³.

2.10 Neurite outgrowth and primary Schwann cell morphology assessment

Four different parameters were analysed for neurite outgrowth as previously described ¹². Image analysis was conducted using a Zeiss LSM Image browser software and Image J (NIH) ¹⁵. The algorithm identified the blue (DAPI / nuclei label) and green (S100 β label) channels to reveal a single red channel image identifying β III tubulin. After conversion to greyscale, images were transferred into Image J (NIH) software and interfaced with a plugin (Neuron J) ^{15,17}. NeuronJ (open source) was used to trace and measure neurites extending from a cell body. Regions of interest were magnified to accurately count the number of neurites extending from the cell body, and for areas where neurite crossed over. The average Schwann cell length was calculated as previously described ¹⁸ using the ruler tool, and aspect ratio calculated using the Analyze Particles tool, on NIH Image J, once images had been manually thresholded ^{15,19}.

2.11 Statistical analysis – GraphPad Instat (GraphPad Software, USA) was used to perform statistical analysis. One-way analysis of variance (ANOVA; $p < 0.05$) was conducted to analyse the differences between data sets incorporating Tukey's multiple comparisons test if $p < 0.05$. Two-way analysis of variance ($p < 0.05$) was conducted to analyse the differences between data sets when assessing live/dead cell numbers incorporating a Sidak's multiple comparisons test if $p < 0.05$. Data was

reported as mean \pm SD, $p < 0.05$. Each experiment was performed three independent times with each sample repeated three times as $n=3$.

3 RESULTS

3.1 Silane modification increases water contact angle - Contact angle results confirmed aminosilane deposition to glass substrates increased surface hydrophobicity (Figure 1). The water contact angle of plain glass ($60 \pm 4^\circ$) significantly increased to $86 \pm 1^\circ$ and $81 \pm 2^\circ$ when grafting SC and LC aminosilanes, respectively. Values recorded were consistent with previously published data, confirming addition of NH_2 silanes to glass ¹⁰.

3.2 Elemental confirmation of silane modification - Elemental analysis by XPS confirmed that aminosilane modified surfaces were enriched with carbon and nitrogen and conversely exhibited decreased silicon and oxygen surface functional content. This demonstrated that aminosilanes were chemically grafted on to glass substrates successfully and consistent with previously published data confirming the presence of $-\text{NH}_2$ modification (Table 1) ¹⁰.

3.3 Silane modification increases surface roughness and elastic modulus - AFM micrographs of plain glass substrates and SC aminosilane surfaces (Figure 2A and B) showed a patchy pattern in roughness and amine deposition. In contrast, LC surfaces had a more homogenous roughness and amine deposition. This observation was in line with our previously findings ¹⁰. The elastic modulus of plain glass (10820 ± 1492 MPa) was significantly decreased when modified with SC aminosilane (8906 ± 51 MPa) and LC aminosilanes (6697 ± 50 MPa) (Figure 2D). In

addition, the LC aminosilane modulus was significantly lower compared to modification using SC aminosilanes.

3.4 Long chain aminosilane supports NG108-15 neuronal cell adhesion and

cell viability - The effect of silane chain length on NG108-15 neuronal cell viability was investigated. Confocal images (Figure 3A-E) identified that NG108-15 neuronal cells attached to all surfaces. Figure 3F showed that significantly higher numbers of live cells were observed on LC aminosilane surfaces (448.9 ± 55.0 cells) compared to SC surfaces and plain glass control (293.4 ± 11.6 and 323.4 ± 11.0 cells), respectively. The highest numbers of live NG108-15 cells were identified when grown on the fibronectin modified surface (478.3 ± 93.4). Cell viabilities of >95% were detected on both aminosilane modified surfaces, deeming them biocompatible, with no differences identified between experimental groups ²⁰.

3.5 Long chain aminosilane supports NG108-15 neuronal cell differentiation -

NG108-15 neuronal cells were cultured on all modified surfaces (Figure 4A-E) were labelled for β III-tubulin to quantify neurite formation. The percentage of neuronal cells bearing neurites was $73.6 \pm 12.2\%$, $68.2 \pm 15.6\%$ and $70.4 \pm 7.6\%$, on the LC, SC and fibronectin modified surfaces compared to plain glass and TCP, $67.9 \pm 10.5\%$, $61.8 \pm 8.8\%$, respectively. No significant differences were detected between data. Neurite outgrowth per neuronal cell significantly increased when cultured on LC and fibronectin surfaces, compared to glass (1.6 ± 0.1 and 1.5 ± 0.07 compared to 1.3 ± 0.1) (Figure 4G). Significantly higher numbers of neurites present per neuron were observed on LC surfaces compared to SC modified surfaces (1.6 ± 0.1 compared to 1.4 ± 0.1). The longest average neurite lengths were observed on TCP control and LC surfaces, $107.1 \pm 9.1\mu\text{m}$ and $98.6 \pm 5.5\mu\text{m}$, respectively. Average

neurite lengths on LC surfaces were significantly longer cell neurites on plain glass surfaces. However, no significant difference was detected between neurite lengths cultured on LC versus SC modified surfaces. Maximum neurite length of 110.2 μm was measured on the LC modified surfaces.

3.6 Aminosilanes support primary Schwann cell viability - All surfaces supported primary Schwann cell attachment, with few dead cells observed (Figure 5A-E). The number of live Schwann cells growing on LC surfaces was higher than on SC aminosilanes, fibronectin coated surfaces and plain glass, (306.2 ± 69.0 cells compared to 348.7 ± 55.3 , 327.2 ± 46.9 and 306.2 ± 68.9 cells respectively). No significant differences were detected between the surfaces when expressed as percentage viability (Figure 5G). All surfaces supported > 95% cell viability.

3.7 Long Chain aminosilane supports primary Schwann cell phenotype -

Primary Schwann cells were cultured on surfaces for 7 days and stained for S100 β , p75NGFR and GFAP (figure 6A-O). All surfaces supported Schwann cell attachment, spreading and growth. Average Schwann cell lengths on SC and LC surfaces and fibronectin coated surfaces were $87.5 \pm 9.8\mu\text{m}$, $83.4 \pm 15.7\mu\text{m}$ and $85.2 \pm 5.6\mu\text{m}$, respectively. Average lengths on glass and TCP was $79.2 \pm 13.4\mu\text{m}$ and $74.1 \pm 10.9\mu\text{m}$, respectively (figure 6P). The aspect ratio (length:width) of Schwann cells cultured on LC, fibronectin coated surfaces and TCP control was significantly higher compared to Schwann cells cultured on SC and glass ($8.1 \pm 2.5\mu\text{m}$, $6.5 \pm 2.1\mu\text{m}$, and $5.6 \pm 2.1\mu\text{m}$, compared to $2.6 \pm 0.8\mu\text{m}$ and $3.1 \pm 0.9\mu\text{m}$) (figure 6Q). Schwann cells exhibited a more polygonal morphology, when cultured on plain and SC modified glass, whereas cells cultured on LC and fibronectin coated glass showed an elongated bipolar phenotype.

3.8 Long chain aminosilane supports primary neuron and Schwann cell

adhesion, and supports primary neuron differentiation - Higher numbers of

Schwann cells were observed on SC and LC modified glass and fibronectin coated glass, compared to plain glass which was patchy (figure 7A-D) . Neurons established more inter-neuron connections when cultured on LC modified and fibronectin coated surfaces, compared to the other surfaces. Neurons cultured on LC and SC surfaces developed significantly higher numbers of neurites (4.7 ± 0.5 neurites and 4.5 ± 0.4 neurites per neuron), compared to cells grown on glass control (3.3 ± 0.4 neurites per neuron; Figure 7F). Neurons cultured on fibronectin and TCP had an average of 4.3 ± 0.4 and 4.2 ± 0.5 neurites per neuron. Neurites from primary neurons cultured on LC surfaces were significantly longer compared to all other surfaces except fibronectin (Figure 7G). The average length of neurites measured on LC modified surfaces and fibronectin coated surfaces were $429.2 \pm 36.6\mu\text{m}$ and $401.3 \pm 67.9\mu\text{m}$ respectively. The maximum neurite length, $557.3\mu\text{m}$, was measured on the LC modified surfaces (Figure 7H).

4 DISCUSSION

Previous studies have demonstrated that changing the chain length of silane changes the surface topography of a substrate, via deposition of amine groups, therefore controlling initial cell adhesion and influencing cellular differentiation ⁹.

Silane chain length has been previously shown to control osteo-induced differentiation of mesenchymal stem cells, and a similar effect was hypothesised for neuronal cell differentiation ¹⁰. The present study investigated two different $-\text{NH}_2$

presenting silane chain lengths: 3-aminopropyl triethoxysilane (SC) and 11-aminoundecyltriethoxysilane (LC) as potential coatings in peripheral nerve repair. Silane modification significantly changed the surface properties of glass, increasing water contact angles compared to the unmodified glass control (Figure 1). The addition of amine groups to a surface, has been well reported to increase hydrophilicity of a surface, decreasing water contact angle²¹. However, Crespin *et al.* reported an increase in water contact angle when modifying clean glass substrates with allylamine, compared to clean glass substrates alone²². The presence of methylene bridges in the aminosilane chains, and change in surface roughness, increased hydrophobicity and was comparable with other published studies^{9, 10}. Overall all surfaces were deemed hydrophilic, with contact angles less than 90°. Modification of substrates was confirmed via XPS analysis, which demonstrated an increase in carbon and nitrogen, and a decrease in silicon and oxygen functional groups (Table 1). Of interest, the 3-aminopropyl triethoxysilane (SC) modified surface demonstrated a higher nitrogen content, compared to the 11-aminoundecyltriethoxysilane (LC) modified surface, suggesting a greater amino group density. This is contrary to previous studies that suggests lower chain SAMs demonstrate better packing due to greater molecular order, and interactions between SAM chains²³. However, our previous study confirmed, using a ninhydrin assay, that 11-aminoundecyltriethoxysilane (LC) modified surfaces had a greater deposition, and density, of –NH₂ groups compared to 3-aminopropyl triethoxysilane (SC) modified surfaces¹⁰. This could be due to higher hydrophobic interaction among the long –CH₂– chain which made the amine groups in LC modified surface to be oriented outwards, which was observed in our previous study¹⁰. The orient of amine

groups in SC modified surfaces was random, due to no/lower hydrophobic interaction among the molecules.

Changes in nanotopography were confirmed by AFM analysis by varying silane chain length (Figure 2). Our previous study¹⁰ illustrated that grafting LC aminosilanes onto substrates increased surface roughness, and was consistent over the entire surface, depositing amine groups as a homogenous layer. Although surface roughness of substrates increased when grafting the SC aminosilane, roughness was patchy when compared to LC aminosilane. Rougher surface topographies have been shown to increase protein adsorption due to increased surface area, which in turn is reported to influence initial cell adhesion, and differentiation²⁴. Aminosilane addition to glass substrates significantly decreased the elastic modulus of clean glass substrates when modifying the surface with LC aminosilane. However, literature suggests the addition of 3-aminopropyl triethoxysilane to substrates, and increasing the concentration, increases elastic modulus²⁵. Tang *et al.* grafted three different aminosilanes, 3-aminopropyltriethoxysilane, N-(2-aminoethyl)-3-aminopropyltrimethoxysilane (A1120), and 3-[2-(2-aminoethylamino)ethylamino] onto epoxy resin/silica coated substrates²⁶. Grafting all the silane coupling agents significantly improved mechanical properties of the epoxy resin, but using the middle chain length aminosilane, N-(2-aminoethyl)-3-aminopropyltrimethoxysilane, reported better improved thermo-mechanical properties²⁶.

Recent studies have shown that cells of the peripheral nervous system are mechanosensitive²⁷. Rosso *et al.* reported significantly higher Schwann cell attachment and neurite outgrowth from DRGs on stiffer substrates (20KPa) compared to softer substrates (1 and 10 KPa)²⁸ and Kayal *et al.* reported that

NG108-15 cell neurite outgrowth directionality could be controlled by substrate stiffness ²⁷. However, it is difficult to compare our results with those of previously reported studies due to the magnitude in size of the DMT moduli reported for the clean glass, SC and LC modified surfaces, as well as differences in substrates modified. Future work will investigate these findings further.

All surfaces supported NG108-15 neuronal cell adhesion and viability. However, significantly higher numbers of live cells were observed adhering to LC modified surfaces compared to SC surfaces, and plain glass, suggesting LC aminosilane preferentially support NG108-15 neuronal cell viability. This agrees with the study by Buttiglione *et al.* whereby the addition of amine groups to PET surfaces, using plasma polymerisation, promoted SY5Y cell adhesion, increasing the surface charge of the substrate and increasing cellular adhesion via electrostatic attraction ²⁹. Albumin, present in cell culture medium, has a higher affinity to both hydrophobic and rough surfaces which would explain the increased number of live cells attached to the LC modified surfaces ³⁰.

This study has shown that the LC aminosilane preferentially supports NG108-15 neuronal cell differentiation consistently across an exposed surface area, compared to the SC modified and plain glass coverslips. NG108-15 neuronal cells were chosen for this study as they have been used for *in vitro* experiments in many peripheral nerve regeneration publications and are indicative of primary neuron responses ³¹. NG108-15 neuronal cells extended significantly higher numbers of neurite-like processes per cell body, as well as significantly longer neurites when cultured on the LC modified surfaces in comparison to cells grown on SC aminosilanes or plain glass. Similar results were observed in Hopper *et al.* in which the addition of amine functionalised nano-diamond promoted NG108-15 cell

differentiation confirmed by an increase in NG108-15 neuronal cell bearing neurites and increase in average neurite length ³². Lizarraga-Valderrama *et al.* also reported that rougher surface topographies induced NG108-15 cell differentiation³³. The addition of LC aminosilane to glass substrates significantly increased average NG108-15 neuronal cell neurite outgrowth lengths and maximum neurite length. In addition to increasing surface roughness, the LC aminosilane could be providing chemical, and physical guidance cues, increasing neurite length. Chemical and physical guidance cues increase cell attachment, proliferation and differentiation, increasing neurite length of neurites outgrown from both NG108 neuronal cells and DRG explants ¹.

Amine modified surfaces supported Schwann cell attachment and cell viability. This was also observed in the study by Li *et al.* who reported that increasing the amount SC aminosilane used for modifying chitosan scaffolds increased primary Schwann cell attachment and proliferation ¹¹. Schwann cells cultured on all surfaces stained positively for GFAP, P75NGFR and S100 β antigens and Schwann cells cultured on LC modified glass exhibited and maintained a typical elongated phenotype, whereas cells cultured on the SC and plain glass surfaces exhibited a polygonal shape ¹⁸. This was quantified by calculating the aspect ratio of Schwann cells cultured on all surfaces, and was significantly higher on the LC surfaces compared to the aspect ratio of Schwann cells cultured on the plain and short chain modified glass. This observation was also reported by Hopper *et al.* in which typical elongated Schwann cells were observed on amine functionalised nano-diamond surfaces, and polygonal shaped Schwann cells observed on acrylic acid coated surfaces ³².

Surface modification of glass, using LC aminosilanization, has also been shown to preferentially support primary neuronal cell and Schwann cell attachment, and primary neuronal cell differentiation. Compared to plain glass, both SC and LC aminosilanes supported neuronal cell differentiation, identified by a significant increase in the average number of neurites per cell. However, the average neurite lengths of neurites extending from primary neurons were significantly longer when cultured on LC aminosilanes, compare to neurons grown on SC aminosilanes or plain glass. Previous studies have reported that the use of amine chemical reactive groups has been shown to increase neuronal cell differentiation^{32,34}. Naka *et al.* reported that patterned self assembling monolayers (SAMs), with amino terminal groups, promoted neurite outgrowth of embryonic chick DRG neurons and PC12 cells compared to SAMs with methyl and carboxyl groups³³. Ren *et al.* also reported that NH₂ modified glass surfaces induced differentiation of neural stem cells, compared to control groups³⁴.

Both LC and SC aminosilanes supported primary neuronal cell differentiation, identified by a significant increase in the average number of neurites sprouting from each neuron. This effect was not observed using NG108-15 cells. Although it is reported that NG108-15 cells can be indicative of primary neuron responses, data gathered is not always comparable to the *in vivo* response³⁶. This study opted to use dissociated DRGs as a primary cell model, to reduce the amount of animal usage (in line with the 3Rs) and obtain results indicative of the *in vivo* response¹². It was observed that primary Schwann cells were always in close proximity to neurite outgrowth which is important for nerve regeneration studies to observe neuronal cell-glia cell connections due to the role that Schwann cells have in nerve repair *in vivo*¹⁸. This study supports the value of more relevant cell sources, such as the

dissociated DRGs for neuronal and Schwann cell studies, highlighting differences between primary cell versus immortal cell lines for investigation of novel biomaterials in peripheral nerve repair.

In summary, we report on a surface deposition method with a LC aminosilane that increases hydrophobicity, surface roughness. This has the effect of supporting cell differentiation as determined by NG108-15 neuronal cells, and primary neurons cultured from dissociated DRGs. Both the SC and LC aminosilanes have been extensively characterised in our previous work and modification of glass substrates for neuronal cell differentiation was comparable to previous studies¹⁰. This is the first study to show that neuronal cell differentiation varies according to the length of the silane chain used. It also highlights the potential of silane modification as a scalable, cost effective approach, compared to using expensive ECM proteins, to functionalise existing biomaterials, used for neurosurgical scaffolds, with amine group surface modification for enhancing neuronal cell differentiation and supporting neuronal and Schwann cell viability.

ACKNOWLEDGEMENTS

We are grateful to Dr Nicola Green for experimental advice and assistance with confocal microscopy at the University of Sheffield (U.K.) Kroto Research Institute Confocal Imaging Facility.

ADDITIONAL INFORMATION

The authors do not have any competing financial interests associated with this work.

Conflict of Interest : None

Data Availability Statement: The data that support the findings of this study are openly available in figshare at <http://doi.org/10.15131/shef.data.13298195>, reference number 13298195.

REFERENCES

1. Bell, J.H. & Haycock, J.W. Next generation nerve guides: materials, fabrication, growth factors, and cell delivery. *Tissue Eng Part B Rev* 2012;18:116-128.
2. Behbehani, M., Glen, A., Taylor, C.S., Schuhmacher, A., Claeysens, F. & Haycock, J.W. Pre-clinical evaluation of advanced nerve guide conduits using a novel 3D in vitro testing model. *Inter J. of Bioprinting* 2018;4.
3. Daly, W., Yao, L., Zeugolis, D., Windebank, A. & Pandit, A. A biomaterials approach to peripheral nerve regeneration: bridging the peripheral nerve gap and enhancing functional recovery. *J R Soc Interface* 2012;9:202-221.
4. Chua, P.K., Chena, J.Y., Wang, L.P. & Huang, N. Plasma-surface modification of biomaterials. *Materials Science and Engineering R* 2002;36:143–206.
5. Curran, J.M., Chen, R. & Hunt, J.A. Controlling the phenotype and function of mesenchymal stem cells in vitro by adhesion to silane-modified clean glass surfaces. *Biomaterials* 2005;26:7057-7067.
6. Buttiglione, M., Vitiello, F., Sardella, E., Petrone, L., Nardulli, M., Favia, P., d'Agostino, R. & Gristina, R. Behaviour of SH-SY5Y neuroblastoma cell line grown in different media and on different chemically modified substrates. *Biomaterials* 2007;28:2932-2945.
7. Ni, H.C., Lin, Z.Y., Hsu, S.H. & Chiu, I.M. The use of air plasma in surface modification of peripheral nerve conduits. *Acta Biomater* 2010;6:2066-2076.

8. Ratner, B.D. Plasma deposition for biomedical applications: a brief review. *J Biomater Sci Polym Ed* 1992;4:3-11.
9. Fawcett, S.A., Curran, J.M., Chen, R., Rhodes, N.P., Murphy, M.F., Wilson, P., Ranganath, L., Dillon, J.P., Gallagher, J.A. & Hunt, J.A. Defining the Properties of an Array of -NH₂-Modified Substrates for the Induction of a Mature Osteoblast/Osteocyte Phenotype from a Primary Human Osteoblast Population Using Controlled Nanotopography and Surface Chemistry. *Calcif Tissue Int* 2017;100:95-106.
10. Chen, R., Hunt, J.A., Fawcett, S., D'sa, R., Akhtar, R. & Curran, J.M. The optimization and production of stable homogeneous amine enriched surfaces with characterized nanotopographical properties for enhanced osteoinduction of mesenchymal stem cells. *J Biomed Mater Res Part A* 2018;106A:1862-1877.
11. Li, G., Zhang, L., Wang, C., Zhao, X., Zhu, C., Zheng, Y., Wang, Y., Zhao, Y. & Yang, Y. Effect of silanization on chitosan porous scaffolds for peripheral nerve regeneration. *Carbohydrate Polymers* 2014;101:718-726.
12. Daud, M.F., Pawar, K.C., Claeysens, F., Ryan, A.J. & Haycock, J.W. An aligned 3D neuronal-glial co-culture model for peripheral nerve studies. *Biomaterials* 2012;33:5901-5913.
13. Kaewkhaw, R., Scutt, A.M. & Haycock, J.W. Integrated culture and purification of rat Schwann cells from freshly isolated adult tissue. *Nat Protoc* 2012;7:1996-2004.
14. de Luca, A.C., Faroni, A. & Reid, A.J. 2015 Dorsal Root Ganglia Neurons and Differentiated Adipose-derived Stem Cells: An In Vitro Co-culture Model to Study Peripheral Nerve Regeneration. *Journal of Visualized Experiments* 2015;52543.
15. Schneider, C.A., Rasband, W.S. & Eliceiri, K.W. NIH Image to ImageJ: 25 years of image analysis. *Nature Methods* 2012;9:671.

16. Usaj, M., Torkar, D., Kanduser, M. & Miklavcic, D. Cell counting tool parameters optimization approach for electroporation efficiency determination of attached cells in phase contrast images. *Journal of Microscopy* 2010;241:303-314.
17. Popko, J., Fernandes, A. & Lanier, L.M. Automated Analysis of NeuronJ Tracing Data. *Cytometry Part A : the journal of the International Society for Analytical Cytology* 2009;75:371-376.
18. Kaewkhaw, R., Scutt, A.M. & Haycock, J.W. Anatomical site influences the differentiation of adipose-derived stem cells for Schwann-cell phenotype and function. *Glia* 2011;59:734-749.
19. Zheng J, Kontoveros D, Lin F, Hua G, Reneker DH, Becker ML, Willits RK. Enhanced Schwann cell attachment and alignment using one-pot "dual click" GRGDS and YIGSR derivatized nanofibers. *Biomacromolecules* 2015;12;16(1):357-63.
20. T, C.S, Cost Effective Optimised Synthetic Surface Modification Strategies for Enhanced Control of Neuronal Cell Differentiation and Supporting Neuronal and Schwann cell Viability, 2020, 10.15131/shef.data.13298195
21. Lee, J.Y. & Schmidt, C.E. Amine-functionalized polypyrrole: Inherently cell adhesive conducting polymer. *J Biomed Mater Res Part A* 2015;103:2126-2132.
22. Crespin M, Moreau N, Masereel B, Feron O, Gallez B, Vander Borght T, Michiels C, Lucas S. Surface properties and cell adhesion onto allylamine-plasma and amine-plasma coated glass coverslips. *J Mater Sci Mater Med* 2011;22(3):671-82.
23. Love, J. C., Estroff, L. A., Kriebel, J. K., Nuzzo, R. G. & Whitesides, G. M. Self-Assembled Monolayers of Thiolates on Metals as a Form of Nanotechnology. *Chemical Reviews* 2005;105:1103-1170.

24. Anselme, K., Ploux, L. & Ponche, A. Cell/Material Interfaces: Influence of Surface Chemistry and Surface Topography on Cell Adhesion. *Journal of Adhesion Science and Technology* 2010;24:831-852.
25. Khan, R. A., Parsons, A. J., Jones, I. A., Walker, G. S. & Rudd, C. D. Effectiveness of 3-Aminopropyl-Triethoxy-Silane as a Coupling Agent for Phosphate Glass Fiber-Reinforced Poly(caprolactone)-based Composites for Fracture Fixation Devices. *Journal of Thermoplastic Composite Materials* 2011;24:517-534.
26. Tang, Y., Tang, C., Hu, D. & Gui, Y. Effect of Aminosilane Coupling Agents with Different Chain Lengths on Thermo-Mechanical Properties of Cross-Linked Epoxy Resin. *Nanomaterials (Basel, Switzerland)* 8, 951, doi:10.3390/nano8110951 (2018).
27. Kayal, C., Moeendarbary, E., Shipley, R.J. & Phillips, J.B. Mechanical Response of Neural Cells to Physiologically Relevant Stiffness Gradients. *Advanced Healthcare Materials* 2019;1901036.
28. Rosso, G., Liashkovich, I., Young, P., Röhr, D. & Shahin, V. Schwann cells and neurite outgrowth from embryonic dorsal root ganglions are highly mechanosensitive. *Nanomedicine: Nanotechnology, Biology and Medicine* 2017;13:493-501.
29. Metwalli, E., Haines, D., Becker, O., Conzone, S. & Pantano, C.G. Surface characterizations of mono-, di-, and tri-aminosilane treated glass substrates. *J Colloid Interface Sci* 2006;298:825-831.
30. Lukasiewicz, B., Basnett, P., Nigmatullin, R., Matharu, R., Knowles, J.C. & Roy, I. Binary polyhydroxyalkanoate systems for soft tissue engineering. *Acta Biomaterialia* 2018;71:225-234.

31. Armstrong, S.J., Wiberg, M., Terenghi, G. & Kingham, P.J. ECM molecules mediate both Schwann cell proliferation and activation to enhance neurite outgrowth. *Tissue Eng* 2007;13:2863-2870.
32. Hopper, A.P., Dugan, J.M., Gill, A.A., Fox, O.J., May, P.W., Haycock, J.W. & Claeysens, F. Amine functionalized nanodiamond promotes cellular adhesion, proliferation and neurite outgrowth. *Biomed Mater* 2014;9:045009.
33. Lizarraga-Valderrama, L.R., Nigmatullin, R., Taylor, C., Haycock, J.W., Claeysens, F., Knowles, J.C. and Roy, I. (2015), Nerve tissue engineering using blends of poly(3-hydroxyalkanoates) for peripheral nerve regeneration. *Eng. Life Sci* 2015;612-621.
34. Ren, Y.-J., Zhang, H., Huang, H., Wang, X.-M., Zhou, Z.-Y., Cui, F.-Z. & An, Y.-H. In vitro behavior of neural stem cells in response to different chemical functional groups. *Biomaterials* 2009;30:1036-1044.
35. Naka, Y., Eda, A., Takei, H. & Shimizu, N. Neurite outgrowths of neurons on patterned self-assembled monolayers. *Journal of Bioscience and Bioengineering* 2002;94:434-439.
36. Rayner, M.L.D., Laranjeira, S., Evans, R.E., Shipley, R.J., Healy, J. & Phillips, J.B. Developing an In Vitro Model to Screen Drugs for Nerve Regeneration. *Anat Rec* 2018;301:1628-1637.

FIGURE LEGENDS

FIGURE 1 - Dynamic water contact angle of glass, short chain (SC) and long chain (LC) aminosilane modified surfaces. Water contact angle significantly increased with addition of the aminosilanes compared to the plain glass control (mean \pm SD, n = 4 independent experiments; ***p < 0.001 and ****p < 0.0001 compared to plain glass).

FIGURE 2 - AFM analysis with scan size $1.4\mu\text{m} \times 1.4\mu\text{m}$: (A) Plain glass control; (B) SC aminosilane modified glass; (C) LC aminosilane modified glass; (D) elastic modulus of aminosilane-modified glass substrates (mean \pm SD, $n=3$; $*p<0.05$ and $**p<0.01$).

FIGURE 3 - Confocal micrographs illustrating NG108-15 neuronal cell viability cultured on: A) fibronectin control; B) Plain glass; C) SC aminosilane; D) LC aminosilane; and E) tissue culture plastic control. Scale bar = $100\mu\text{m}$. Cells labelled with syto 9 (green= live cells) and propidium iodide (red= dead cells). F) Number of live cells versus dead cells per sample (mean \pm SD, $n=3$ independent experiments; $P< 0.05$, $**p<0.01$, $***p<0.001$ and $****p<0.0001$) and G) live cell analysis expressed as percentage (mean \pm SD, $n=3$ independent experiments; $P< 0.05$).

FIGURE 4 - Confocal micrographs of NG108-15 neuronal cells immunolabelled for β III-tubulin and DAPI on: A) fibronectin control; B) Plain glass; C) SC aminosilane; D) LC aminosilane; and E) tissue culture plastic control. Scale bar = $100\mu\text{m}$. Confocal images were quantified to determine: F) The percentage of neurite bearing neuronal cells after 6 days in culture (mean \pm SD, $n=3$; $p<0.05$); G) the average number of neurites expressed per neuron (mean \pm SD, $n=3$; $*p<0.05$ and $**p<0.01$) and H) average neurite length per condition after 6 days in culture (mean \pm SD, $n=3$; $*p<0.05$, $**p<0.01$ and $***p<0.001$). I) Maximum neurite length on all substrates.

FIGURE 5 - Confocal micrographs showing live/dead analysis of primary rat Schwann cells on: A) fibronectin control; B) Plain glass; C) SC aminosilane; D) LC aminosilane; and E) tissue culture plastic control. Scale bar = $100\mu\text{m}$. F) Number of live cells versus dead cells per sample and G) live cell analysis expressed as a percentage (mean \pm SD, $n=3$ independent experiments).

FIGURE 6 - Confocal micrographs of primary rat Schwann cells immunolabelled for S100 β (green), GFAP (red) and P75NGFR (yellow) after 6 days of culture on fibronectin controls, plain glass, SC and LC aminosilanes, and tissue culture plastic. Schwann cells were immunolabelled to confirm Schwann cell phenotype. P)

Average Schwann cell length; Q) aspect ratio (length/width) to identify Schwann cell phenotype (mean \pm SD, n=3; *p<0.05).

FIGURE 7 - Confocal micrographs of primary neurons and primary Schwann cells dissociated from dorsal root ganglion bodies and immunolabelled against β -III tubulin (red) and S100 β (green), and cell nuclei (DAPI; blue). Cells were cultured on: A) fibronectin control; B) Plain glass; C) SC aminosilane; D) LC aminosilane; and E) tissue culture plastic control. Scale bar = 100 μ m. F) Average numbers of neurites per neuron after 7 days in culture (mean \pm SD, n=3 *p<0.05 versus plain glass). G) Average neurite length (mean \pm SD, n=3, *p<0.05, **p<0.01, and ***p<0.001, versus LC aminosilane, #p<0.05 versus tissue culture plastic). H) Maximum neurite length on all substrates.

TABLE LEGEND

TABLE 1 – X-ray photoelectron spectroscopy characterization of glass surfaces after aminosilane modification. XPS elemental composition is shown as percentage of carbon, silicon, oxygen and nitrogen for glass control, short chain and long chain aminosilane-modified surfaces (mean \pm SD, n=4).

TABLE 1

Substrate	% Elemental Composition			
	C	Si	O	N
Glass	54.3 ± 2.1	27.5 ± 0.8	17.8 ± 2.1	0
Short Chain	58.3 ± 0	13.2 ± 0.5	19.6 ± 0.1	8.9 ± 0.7
Long Chain	62.1 ± 0.2	11.8 ± 0.3	23.0 ± 0.2	3.1 ± 0.7

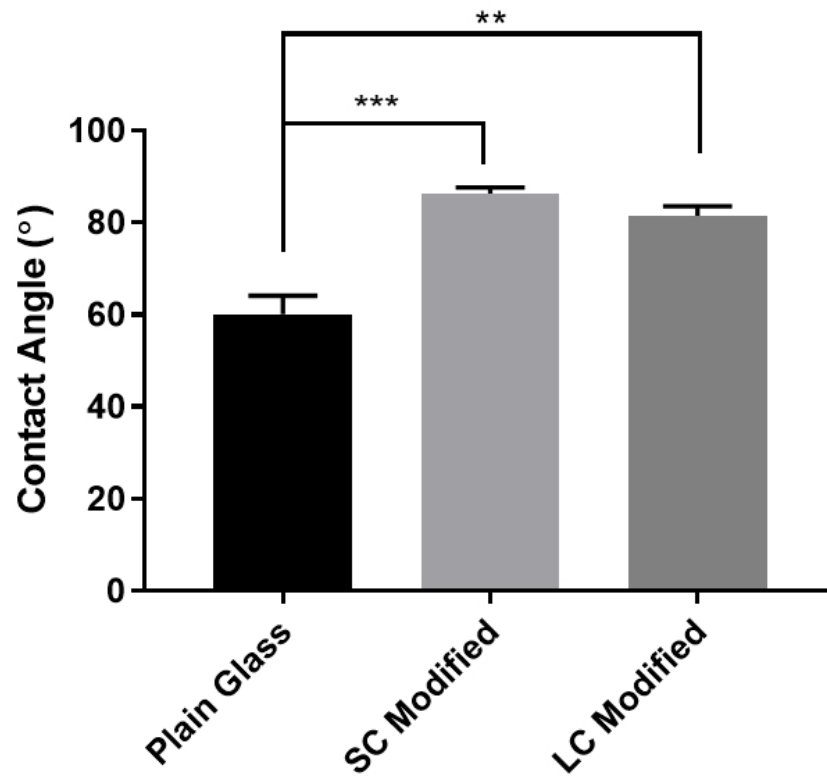


FIGURE 1 - Dynamic water contact angle of glass, short chain (SC) and long chain (LC) aminosilane modified surfaces. Water contact angle significantly increased with addition of the aminosilanes compared to the plain glass control (mean \pm SD, n = 4 independent experiments; ***p < 0.001 and ****p < 0.0001 compared to plain glass).

7x7mm (2400 x 2400 DPI)

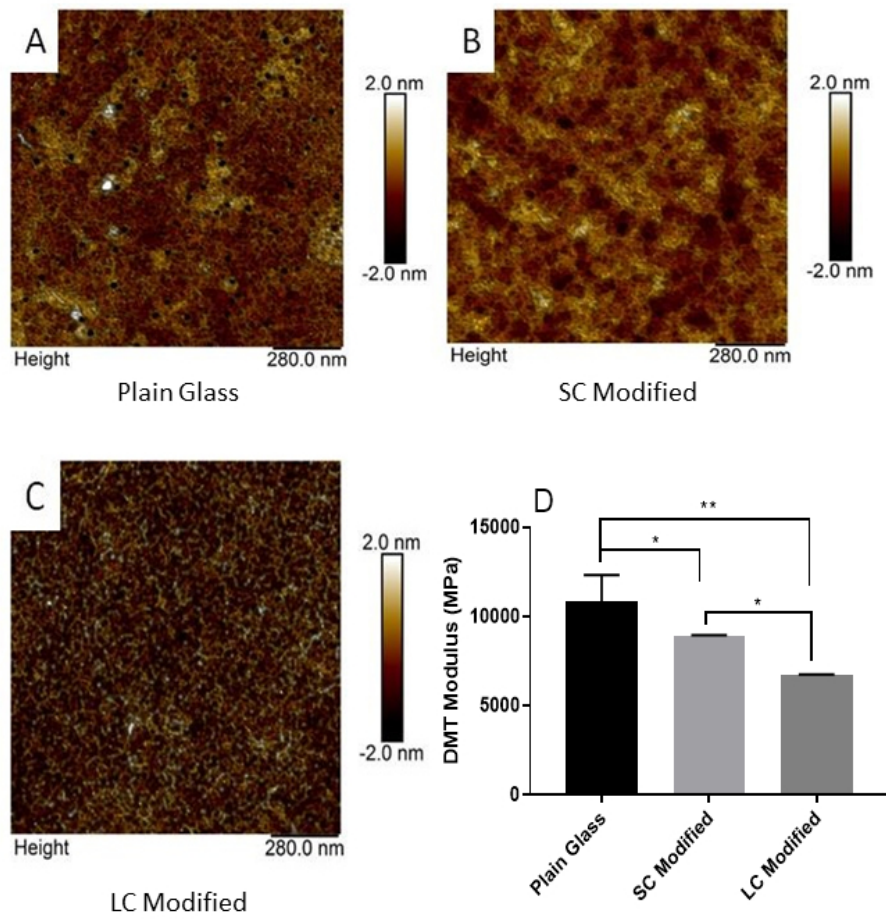


FIGURE 2 - AFM analysis with scan size $1.4\mu\text{m} \times 1.4\mu\text{m}$: (A) Plain glass control; (B) SC aminosilane modified glass; (C) LC aminosilane modified glass; (D) elastic modulus of aminosilane-modified glass substrates (mean \pm SD, $n=3$; * $p<0.05$ and ** $p<0.01$).

15x15mm (1200 x 1200 DPI)

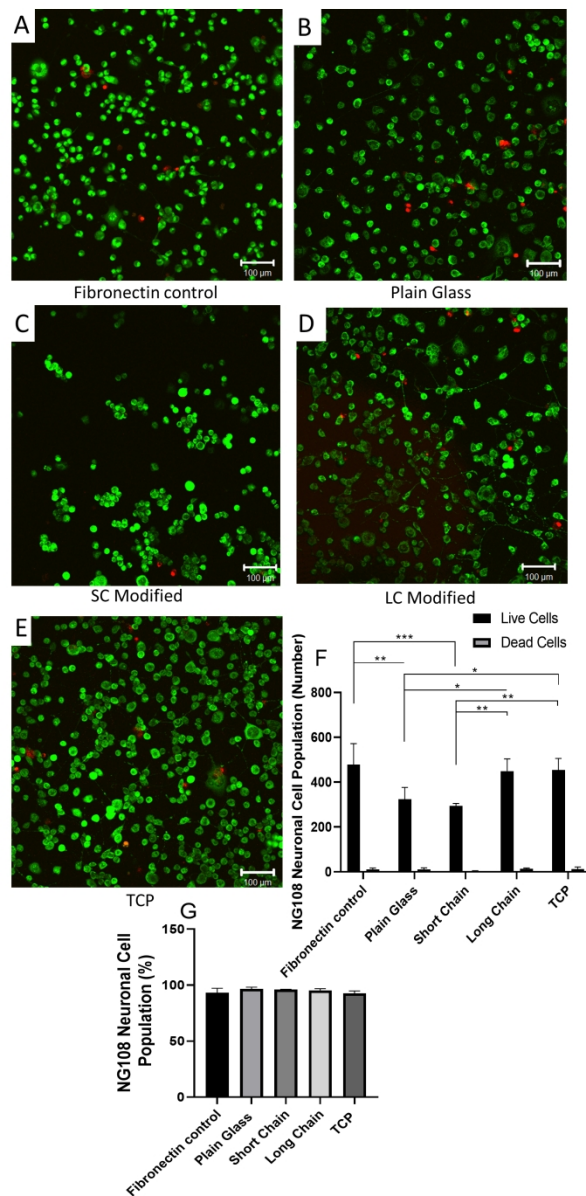


FIGURE 3 - Confocal micrographs illustrating NG108-15 neuronal cell viability cultured on: A) fibronectin control; B) Plain glass; C) SC aminosilane; D) LC aminosilane; and E) tissue culture plastic control. Scale bar = 100 μm. Cells labelled with syto 9 (green= live cells) and propidium iodide (red= dead cells). F) Number of live cells versus dead cells per sample (mean ± SD, n=3 independent experiments; $P < 0.05$, $**p < 0.01$, $***p < 0.001$ and $****p < 0.0001$) and G) live cell analysis expressed as percentage (mean ± SD, n=3 independent experiments; $P < 0.05$).

40x80mm (1200 x 1200 DPI)

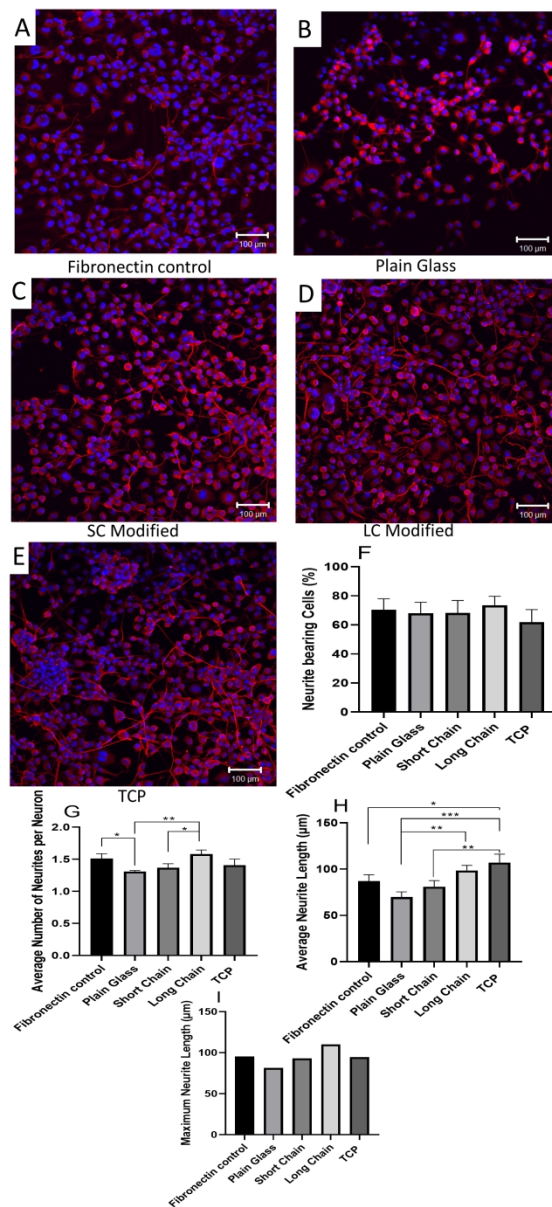


FIGURE 4 - Confocal micrographs of NG108-15 neuronal cells immunolabelled for β III-tubulin and DAPI on: A) fibronectin control; B) Plain glass; C) SC aminosilane; D) LC aminosilane; and E) tissue culture plastic control. Scale bar = 100 μ m. Confocal images were quantified to determine: F) The percentage of neurite bearing neuronal cells after 6 days in culture (mean \pm SD, n=3; p<0.05); G) the average number of neurites expressed per neuron (mean \pm SD, n=3; *p<0.05 and **p<0.01) and H) average neurite length per condition after 6 days in culture (mean \pm SD, n=3; *p<0.05, **p<0.01 and ***p<0.001). I) Maximum neurite length on all substrates.

40x80mm (1200 x 1200 DPI)

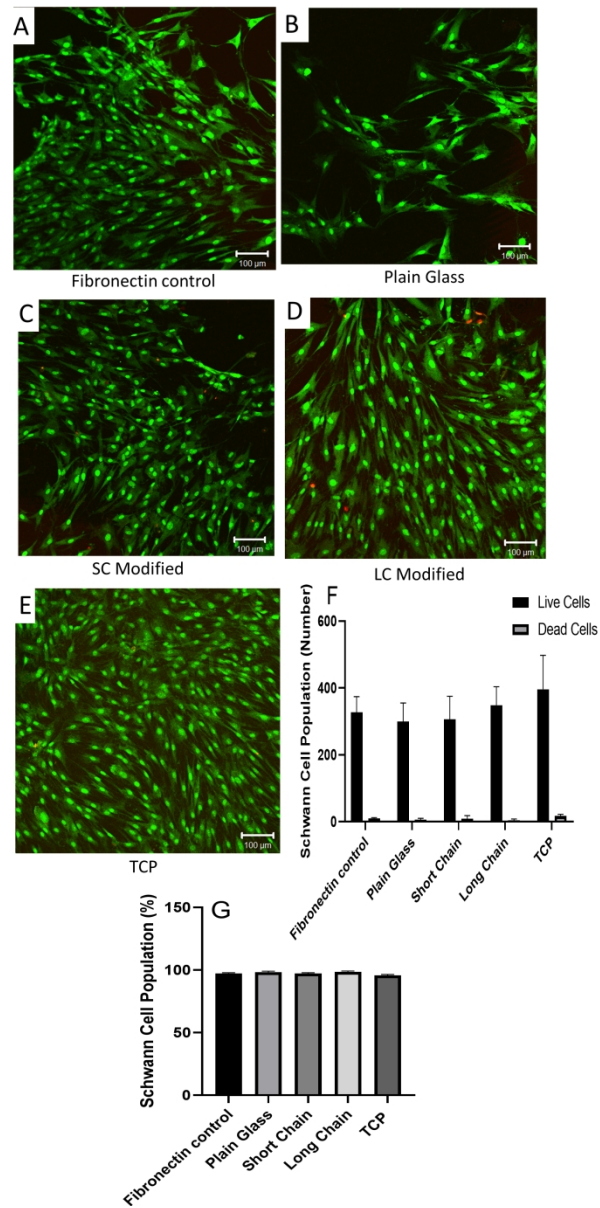


FIGURE 5 - Confocal micrographs showing live/dead analysis of primary rat Schwann cells on: A) fibronectin control; B) Plain glass; C) SC aminosilane; D) LC aminosilane; and E) tissue culture plastic control. Scale bar = 100 μ m. F) Number of live cells versus dead cells per sample and G) live cell analysis expressed as a percentage (mean \pm SD, n=3 independent experiments).

40x80mm (1200 x 1200 DPI)

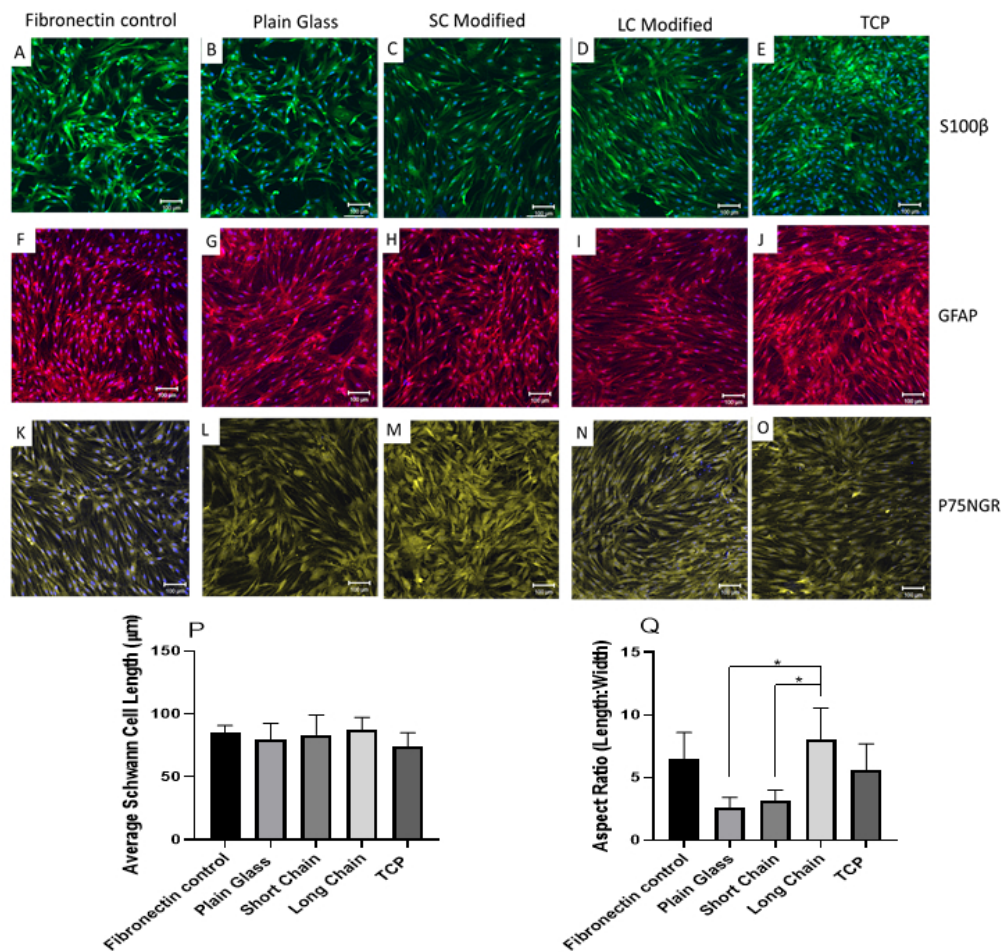


FIGURE 6 - Confocal micrographs of primary rat Schwann cells immunolabelled for S100 β (green), GFAP (red) and P75NGFR (yellow) after 6 days of culture on fibronectin controls, plain glass, SC and LC aminosilanes, and tissue culture plastic. Schwann cells were immunolabelled to confirm Schwann cell phenotype. P) Average Schwann cell length; Q) aspect ratio (length/width) to identify Schwann cell phenotype (mean \pm SD, n=3; *p<0.05).

30x30mm (600 x 600 DPI)

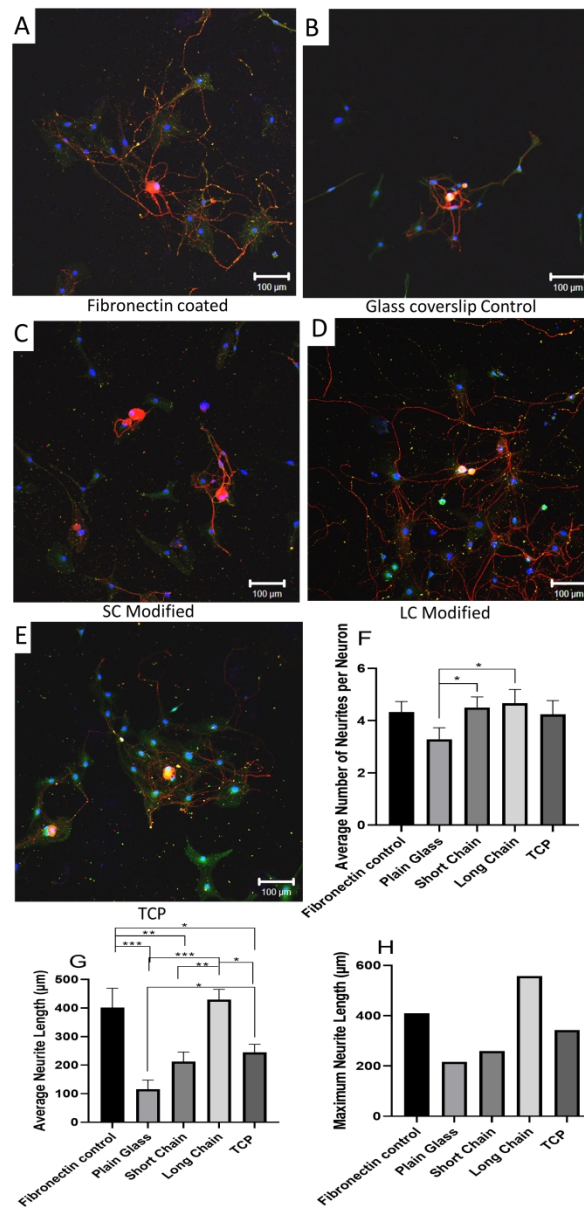


FIGURE 7 - Confocal micrographs of primary neurons and primary Schwann cells dissociated from dorsal root ganglion bodies and immunolabelled against β -III tubulin (red) and S100 β (green), and cell nuclei (DAPI; blue). Cells were cultured on: A) fibronectin control; B) Plain glass; C) SC aminosilane; D) LC aminosilane; and E) tissue culture plastic control. Scale bar = 100 μm . F) Average numbers of neurites per neuron after 7 days in culture (mean \pm SD, n=3 *p<0.05 versus plain glass). G) Average neurite length (mean \pm SD, n=3, *p<0.05, **p<0.01, and ***p<0.001, versus LC aminosilane, #p<0.05 versus tissue culture plastic). H) Maximum neurite length on all substrates.

40x80mm (1200 x 1200 DPI)

Cost Effective Optimised Synthetic Surface Modification Strategies for Enhanced Control of Neuronal Cell Differentiation and Supporting Neuronal and Schwann cell Viability

Caroline S. Taylor^{1*}, Rui Chen², Raechelle D' Sa², John A. Hunt³, Judith M. Curran²
and John W. Haycock^{1*}

¹ Department of Materials Science and Engineering, University of Sheffield, Sheffield,
S3 7HQ. U.K

² Department of Mechanical, Materials and Aerospace, University of Liverpool,
Liverpool, U.K.

³ Medical Technologies and Advanced Materials, Nottingham Trent University,
Nottingham NG11 8NS, U.K.

***CORRESPONDING AUTHORS**

Professor John W. Haycock
Department of Materials Science and Engineering
University of Sheffield
Sheffield
S3 7HQ.
U.K.

Email: j.w.haycock@sheffield.ac.uk

Telephone: +44 (0)114 2225972

Dr Caroline S. Taylor
Department of Materials Science and Engineering
University of Sheffield
Sheffield
S3 7HQ.
U.K.

Email: c.s.taylor@sheffield.ac.uk

ABSTRACT

Enriching a biomaterial surface with specific chemical groups has previously been considered for producing surfaces that influence cell response. Silane layer deposition has previously been shown to control mesenchymal stem cell adhesion and differentiation. However, it has not been used to investigate neuronal or Schwann cell responses *in vitro* to date. We report on the deposition of aminosilane groups for peripheral neurons and Schwann cells studying two chain lengths: 1) 3-aminopropyl triethoxysilane (short chain-SC) and 2) 11-aminoundecyltriethoxysilane (long chain-LC) by coating glass substrates. Surfaces were characterised by water contact angle, AFM and XPS. LC-NH₂ was produced reproducibly as a homogenous surface with controlled nanotopography. Primary neuron and NG108-15 neuronal cell differentiation and primary Schwann cell responses were investigated *in vitro* by S100 β , p75 and GFAP antigen expression. Both amine silane surface supported neuronal and Schwann cell growth, however neuronal differentiation was greater on LC aminosilanes versus SC. Thus, we report that silane surfaces with an optimal chain length may have potential in peripheral nerve repair for the modification and improvement of nerve guidance devices.

KEY WORDS: Peripheral nerve injury; dorsal root ganglion; surface chemistry; amine; silane; surface coating

1 INTRODUCTION

Peripheral nerve injuries affect 7 million people globally every year, and most commonly arise from trauma incidents ¹. Peripheral nerve has the ability to regenerate after injury by a process known as Wallerian degeneration and regeneration ². However, severity of injury determines the success of repair, and surgical intervention usually required ¹. An autograft or synthetic hollow nerve guide

conduit (NGCs) can be used to 'bridge' gaps between the ends of nerve stumps³. Nerve guide conduits are entubulation devices manufactured from both natural and synthetic materials¹, with an emerging number of FDA approved devices comprising hollow tubes, wraps and cuffs. However, nerve guide use is limited to short gap injuries (<20mm) and therefore autograft use is required for large gap injuries, >20mm. Though the current 'gold standard' treatment, autografts are associated with donor site morbidity and there is a lack of donor nerve available². This is focussing attention to NGC designs and methods for improvement, including surface topography and guidance cues for regenerating axons present in autografts³. Approaches used to improve hollow NGCs include the addition of intraluminal guidance scaffolds, incorporating channels and pores, coatings, and changing surface chemistry and topography.

The use of coatings have been shown to improve initial cellular adhesion with synthetic biomaterial surfaces e.g. extra cellular matrix (ECM) proteins¹. ECM coatings mimic native extracellular matrix cues and to an extent surface topography, providing the correct biochemical interactions for adhesion and potentially improving regenerative outcomes of a conduit³. Proteins such as laminin, collagen and fibronectin improve neuronal and Schwann cell adhesion and differentiation when incorporated into bioengineered NGCs¹. For device translation, the use of naturally-derived proteins must consider cost, potential batch variation, and unwanted immune response. Alternatively, synthetic coatings are scalable, reproducible and cost-effective⁴.

Synthetic coatings can control the type, level and conformation of serum proteins that adsorb¹. Alteration of the surface chemistry can influence protein surface conformation, and influence initial adhesion, proliferation and cell

differentiation⁵. Techniques such as plasma polymerisation have been used to alter biomaterial surface chemistry, without altering bulk material properties¹. Plasma deposition studies report on acrylic acid and allyamine surface modification improving SH-SY5Y neuronal cell adhesion and differentiation⁶ and air plasma techniques also increasing primary Schwann cell adhesion onto modified surfaces, increasing nerve regenerative properties of conduits when grafted with peptide or growth factors⁷. However, plasma polymerisation requires a high vacuum, limiting scale-up⁸, supporting a need for simpler surface modification.

Silane modification is a simple, cost effective, controllable and scalable technique for biomaterial modification. Previous work has demonstrated enrichment of surfaces with chemical reactive groups including amines, hydroxyl and carboxyl⁵. Silane modification can mimic the ECM by changing surface nano-topography, and substrate chemistry, providing a biological surface to enhance initial cell attachment and maintain proliferation⁹. Silane chain length has been shown to influence deposition of the chemical reactive group at submicron scale, and influence cell adhesion and differentiation due to topographic profile⁹.

We have previously reported that 11-aminoundecyltriethoxysilane surfaces supported osteogenic differentiation of mesenchymal stem cells, in contrast to 3-aminopropyl triethoxysilane¹⁰. Aminosilanes, of varying chain lengths, were fully characterised, using water contact angle, X-ray photoelectron spectroscopy and atomic force microscopy, to determine the effect of silane chain length on surface chemistry and topography at sub micron level. 11-aminoundecyltriethoxysilane modified surfaces presented an ordered nanoroughness, resulting in favourable 'surface chemistry and topography' for osteoinduction, but has not been investigated for other tissue engineering applications¹⁰.

In the context of nerve repair, one study has reported modifying chitosan using 3-aminopropyl triethoxysilane which promoted increased Schwann cell adhesion and proliferation¹¹. However, silane chain length has not been investigated thoroughly for nerve implant biomaterials. The aim of the present study was to investigate the influence of two different silane chain lengths, with known surface chemistry and topography, characterised from our previous study¹⁰, on neuronal and Schwann cell differentiation and phenotype.

2 MATERIALS AND METHODS

2.1 Preparation and modification of borosilicate glass coverslips - Glass

coverslips (13mm²) were modified with 3% aminosilanes (SC: 3-aminopropyl triethoxysilane; LC: 11-aminoundecyltriethoxysilane) as previously described¹⁰.

Briefly, glass coverslips were cleaned using a 0.5M solution of sodium hydroxide and then 1M Nitric acid for 30 minutes in an ultrasonic bath, followed by washing in three changes of distilled water, and dried in a 50°C oven. Clean coverslips were then modified using the 0.1M silanes, 3-Aminopropyl triethoxysilane (Sigma), and 11-Aminoundecyltriethoxysilane (Fluorochem), in pure isopropanol for 30 minutes. Samples were then rinsed with isopropanol and distilled water. All glass coverslips were sterilised with 70% ethanol for 30 minutes, and washed overnight with PBS before cell culture studies. Prior to cell seeding, 2µg/mL of fibronectin (Merck), in sterile PBS, was added to clean plain glass coverslips, as the control, and incubated at 37°C in 5% CO₂ for 30 minutes.

2.2 Water contact angle measurement - Dynamic contact angles of the samples in deionised purified water were measured using a Dynamic Contact Angle

Tensiometer (CDCA 100, Camtel Ltd., Royston, Herts, UK) at 22 ± 0.5 °C. Briefly, two samples were tightly stuck together on the unmodified side. Each sample was immersed into the wetting solution (deionised pure water) at a rate of 0.060 mm/s. The wetting force at the solid/liquid/vapour interface was recorded by an electrobalance as a function of time and immersion depth and was converted into an advancing contact angle. The values reported for dynamic advancing angles of modified glass coverslips are mean and standard deviations of $n = 4$.

2.3 X-ray photoelectron spectroscopy (XPS) – Elemental surface chemistry, of aminosilane modified substrates, was confirmed using XPS as previously described¹⁰.

2.4 Atomic force microscopy (AFM) - Atomic force microscopy was used to confirm surface topography, previously reported, of the NH₂ modified substrates. AFM was performed as previously described¹⁰. Mechanical properties of silane glass surfaces were investigated by fitting the AFM data obtained with the Derjaguin–Muller–Toporov (DMT) model to extract the elastic modulus of modified glass substrates by fitting the contact region of the retract curve close to the contact point.

2.5 NG108-15 cell culture – An NG108-15 (ECACC 88112303) cell line was used for study. They were originally created from Sendai virus mediated fusion of a mouse neuroblastoma and rat glioma cells. They are a valuable experimental *in vitro* tool for quantifying neurite development as a proxy for primary neuronal cell differentiation. Herein they will be referred to as NG108-15 neuronal cells in this context¹², with experimental culture and conditions used for experiments as

previously described ¹². Cultures were maintained for 6 days, changing the culture medium to serum free Dulbecco's Modified Eagle Medium (DMEM) after 2 days in culture.

2.6 Isolation and culture of primary Schwann cells – Rat primary Schwann cells were isolated and cultured as previously described ¹³. Schwann cells were cultured up to passage 7 for experiments. 60,000 Schwann cells, per sample, were seeded onto surfaces for 6 days and medium replaced once at day 3.

2.7 Isolation and dissociation of dorsal root ganglion bodies (DRGs) -

Dissociation of DRGs into co-cultures of primary neurons and Schwann cells was performed using the methods as previously described ¹⁴. Co-cultures were maintained in F12 medium (containing 2 mM glutamine, 1% penicillin/streptomycin and 0.25% amphotericin B) supplemented with the addition of 100ug/mL bovine serum albumin (BSA), 10 μ L/mL of N₂ and 77ng/mL of nerve growth factor (NGF). Cells were left in culture for 7 days, and medium changed at day 4.

2.8 Live/dead analysis of NG108-15 cells and primary Schwann cells -

Cell viability was confirmed by live/dead analysis, and samples imaged using confocal microscopy as previously described ¹². Cells were counted using a ITCN cell counter plugin on Image J NIH software ^{15, 16}.

2.9 Immunolabelling of NG108-15 cells, Schwann cells and dissociated dorsal

root ganglia – Modified coverslips containing NG108-15 cells only, Schwann cells only, and those containing dissociated DRG cultures, were labelled for cell type specific antigens, and imaged using confocal microscopy as previously described ¹². NG108-15 cells and primary neurons were labelled for β III-tubulin (neurite marker)

and Schwann cells labelled for S100 β in co-culture with primary neurons. Mono-culture of primary Schwann cells on modified substrates were labelled for S100 β , Glial fibrillary acidic protein (GFAP) low-affinity nerve growth factor receptor (p75NGFR) as previously described ¹³.

2.10 Neurite outgrowth and primary Schwann cell morphology assessment

Four different parameters were analysed for neurite outgrowth as previously described ¹². Image analysis was conducted using a Zeiss LSM Image browser software and Image J (NIH) ¹⁵. The algorithm identified the blue (DAPI / nuclei label) and green (S100 β label) channels to reveal a single red channel image identifying β III tubulin. After conversion to greyscale, images were transferred into Image J (NIH) software and interfaced with a plugin (Neuron J) ^{15,17}. NeuronJ (open source) was used to trace and measure neurites extending from a cell body. Regions of interested were magnified to accurately count the number of neurites extending from the cell body, and for areas where neurite crossed over. The average Schwann cell length was calculated as previously described ¹⁸ using the ruler tool, and aspect ratio calculated using the Analyze Particles tool, on NIH Image J, once images had been manually thresholded ^{15,19}.

2.11 Statistical analysis – GraphPad Instat (GraphPad Software, USA) was used to perform statistical analysis. One-way analysis of variance (ANOVA; $p < 0.05$) was conducted to analyse the differences between data sets incorporating Tukey's multiple comparisons test if $p < 0.05$. Two-way analysis of variance ($p < 0.05$) was conducted to analyse the differences between data sets when assessing live/dead cell numbers incorporating a Sidak's multiple comparisons test if $p < 0.05$. Data was

reported as mean \pm SD, $p < 0.05$. Each experiment was performed three independent times with each sample repeated three times as $n=3$.

3 RESULTS

3.1 Silane modification increases water contact angle - Contact angle results confirmed aminosilane deposition to glass substrates increased surface hydrophobicity (Figure 1). The water contact angle of plain glass ($60 \pm 4^\circ$) significantly increased to $86 \pm 1^\circ$ and $81 \pm 2^\circ$ when grafting SC and LC aminosilanes, respectively. Values recorded were consistent with previously published data, confirming addition of NH_2 silanes to glass ¹⁰.

3.2 Elemental confirmation of silane modification - Elemental analysis by XPS confirmed that aminosilane modified surfaces were enriched with carbon and nitrogen and conversely exhibited decreased silicon and oxygen surface functional content. This demonstrated that aminosilanes were chemically grafted on to glass substrates successfully and consistent with previously published data confirming the presence of $-\text{NH}_2$ modification (Table 1) ¹⁰.

3.3 Silane modification increases surface roughness and elastic modulus - AFM micrographs of plain glass substrates and SC aminosilane surfaces (Figure 2A and B) showed a patchy pattern in roughness and amine deposition. In contrast, LC surfaces had a more homogenous roughness and amine deposition. This observation was in line with our previously findings ¹⁰. The elastic modulus of plain glass (10820 ± 1492 MPa) was significantly decreased when modified with SC aminosilane (8906 ± 51 MPa) and LC aminosilanes (6697 ± 50 MPa) (Figure 2D). In

addition, the LC aminosilane modulus was significantly lower compared to modification using SC aminosilanes.

3.4 Long chain aminosilane supports NG108-15 neuronal cell adhesion and

cell viability - The effect of silane chain length on NG108-15 neuronal cell viability was investigated. Confocal images (Figure 3A-E) identified that NG108-15 neuronal cells attached to all surfaces. Figure 3F showed that significantly higher numbers of live cells were observed on LC aminosilane surfaces (448.9 ± 55.0 cells) compared to SC surfaces and plain glass control (293.4 ± 11.6 and 323.4 ± 11.0 cells), respectively. The highest numbers of live NG108-15 cells were identified when grown on the fibronectin modified surface (478.3 ± 93.4). Cell viabilities of >95% were detected on both aminosilane modified surfaces, deeming them biocompatible, with no differences identified between experimental groups ²⁰.

3.5 Long chain aminosilane supports NG108-15 neuronal cell differentiation -

NG108-15 neuronal cells were cultured on all modified surfaces (Figure 4A-E) were labelled for β III-tubulin to quantify neurite formation. The percentage of neuronal cells bearing neurites was $73.6 \pm 12.2\%$, $68.2 \pm 15.6\%$ and $70.4 \pm 7.6\%$, on the LC, SC and fibronectin modified surfaces compared to plain glass and TCP, $67.9 \pm 10.5\%$, $61.8 \pm 8.8\%$, respectively. No significant differences were detected between data. Neurite outgrowth per neuronal cell significantly increased when cultured on LC and fibronectin surfaces, compared to glass (1.6 ± 0.1 and 1.5 ± 0.07 compared to 1.3 ± 0.1) (Figure 4G). Significantly higher numbers of neurites present per neuron were observed on LC surfaces compared to SC modified surfaces (1.6 ± 0.1 compared to 1.4 ± 0.1). The longest average neurite lengths were observed on TCP control and LC surfaces, $107.1 \pm 9.1\mu\text{m}$ and $98.6 \pm 5.5\mu\text{m}$, respectively. Average

neurite lengths on LC surfaces were significantly longer cell neurites on plain glass surfaces. However, no significant difference was detected between neurite lengths cultured on LC versus SC modified surfaces. Maximum neurite length of 110.2 μm was measured on the LC modified surfaces.

3.6 Aminosilanes support primary Schwann cell viability - All surfaces supported primary Schwann cell attachment, with few dead cells observed (Figure 5A-E). The number of live Schwann cells growing on LC surfaces was higher than on SC aminosilanes, fibronectin coated surfaces and plain glass, (306.2 ± 69.0 cells compared to 348.7 ± 55.3 , 327.2 ± 46.9 and 306.2 ± 68.9 cells respectively). No significant differences were detected between the surfaces when expressed as percentage viability (Figure 5G). All surfaces supported > 95% cell viability.

3.7 Long Chain aminosilane supports primary Schwann cell phenotype -

Primary Schwann cells were cultured on surfaces for 7 days and stained for S100 β , p75NGFR and GFAP (figure 6A-O). All surfaces supported Schwann cell attachment, spreading and growth. Average Schwann cell lengths on SC and LC surfaces and fibronectin coated surfaces were $87.5 \pm 9.8\mu\text{m}$, $83.4 \pm 15.7\mu\text{m}$ and $85.2 \pm 5.6\mu\text{m}$, respectively. Average lengths on glass and TCP was $79.2 \pm 13.4\mu\text{m}$ and $74.1 \pm 10.9\mu\text{m}$, respectively (figure 6P). The aspect ratio (length:width) of Schwann cells cultured on LC, fibronectin coated surfaces and TCP control was significantly higher compared to Schwann cells cultured on SC and glass ($8.1 \pm 2.5\mu\text{m}$, $6.5 \pm 2.1\mu\text{m}$, and $5.6 \pm 2.1\mu\text{m}$, compared to $2.6 \pm 0.8\mu\text{m}$ and $3.1 \pm 0.9\mu\text{m}$) (figure 6Q). Schwann cells exhibited a more polygonal morphology, when cultured on plain and SC modified glass, whereas cells cultured on LC and fibronectin coated glass showed an elongated bipolar phenotype.

3.8 Long chain aminosilane supports primary neuron and Schwann cell

adhesion, and supports primary neuron differentiation - Higher numbers of

Schwann cells were observed on SC and LC modified glass and fibronectin coated glass, compared to plain glass which was patchy (figure 7A-D) . Neurons established more inter-neuron connections when cultured on LC modified and fibronectin coated surfaces, compared to the other surfaces. Neurons cultured on LC and SC surfaces developed significantly higher numbers of neurites (4.7 ± 0.5 neurites and 4.5 ± 0.4 neurites per neuron), compared to cells grown on glass control (3.3 ± 0.4 neurites per neuron; Figure 7F). Neurons cultured on fibronectin and TCP had an average of 4.3 ± 0.4 and 4.2 ± 0.5 neurites per neuron. Neurites from primary neurons cultured on LC surfaces were significantly longer compared to all other surfaces except fibronectin (Figure 7G). The average length of neurites measured on LC modified surfaces and fibronectin coated surfaces were $429.2 \pm 36.6\mu\text{m}$ and $401.3 \pm 67.9\mu\text{m}$ respectively. The maximum neurite length, $557.3\mu\text{m}$, was measured on the LC modified surfaces (Figure 7H).

4 DISCUSSION

Previous studies have demonstrated that changing the chain length of silane changes the surface topography of a substrate, via deposition of amine groups, therefore controlling initial cell adhesion and influencing cellular differentiation ⁹.

Silane chain length has been previously shown to control osteo-induced differentiation of mesenchymal stem cells, and a similar effect was hypothesised for neuronal cell differentiation ¹⁰. The present study investigated two different $-\text{NH}_2$

presenting silane chain lengths: 3-aminopropyl triethoxysilane (SC) and 11-aminoundecyltriethoxysilane (LC) as potential coatings in peripheral nerve repair. Silane modification significantly changed the surface properties of glass, increasing water contact angles compared to the unmodified glass control (Figure 1). The addition of amine groups to a surface, has been well reported to increase hydrophilicity of a surface, decreasing water contact angle²¹. However, Crespin *et al.* reported an increase in water contact angle when modifying clean glass substrates with allylamine, compared to clean glass substrates alone²². The presence of methylene bridges in the aminosilane chains, and change in surface roughness, increased hydrophobicity and was comparable with other published studies^{9, 10}. Overall all surfaces were deemed hydrophilic, with contact angles less than 90°. Modification of substrates was confirmed via XPS analysis, which demonstrated an increase in carbon and nitrogen, and a decrease in silicon and oxygen functional groups (Table 1). Of interest, the 3-aminopropyl triethoxysilane (SC) modified surface demonstrated a higher nitrogen content, compared to the 11-aminoundecyltriethoxysilane (LC) modified surface, suggesting a greater amino group density. This is contrary to previous studies that suggests lower chain SAMs demonstrate better packing due to greater molecular order, and interactions between SAM chains²³. However, our previous study confirmed, using a ninhydrin assay, that 11-aminoundecyltriethoxysilane (LC) modified surfaces had a greater deposition, and density, of –NH₂ groups compared to 3-aminopropyl triethoxysilane (SC) modified surfaces¹⁰. This could be due to higher hydrophobic interaction among the long –CH₂– chain which made the amine groups in LC modified surface to be oriented outwards, which was observed in our previous study¹⁰. The orient of amine

groups in SC modified surfaces was random, due to no/lower hydrophobic interaction among the molecules.

Changes in nanotopography were confirmed by AFM analysis by varying silane chain length (Figure 2). Our previous study¹⁰ illustrated that grafting LC aminosilanes onto substrates increased surface roughness, and was consistent over the entire surface, depositing amine groups as a homogenous layer. Although surface roughness of substrates increased when grafting the SC aminosilane, roughness was patchy when compared to LC aminosilane. Rougher surface topographies have been shown to increase protein adsorption due to increased surface area, which in turn is reported to influence initial cell adhesion, and differentiation²⁴. Aminosilane addition to glass substrates significantly decreased the elastic modulus of clean glass substrates when modifying the surface with LC aminosilane. However, literature suggests the addition of 3-aminopropyl triethoxysilane to substrates, and increasing the concentration, increases elastic modulus²⁵. Tang *et al.* grafted three different aminosilanes, 3-aminopropyltriethoxysilane, N-(2-aminoethyl)-3-aminopropyltrimethoxysilane (A1120), and 3-[2-(2-aminoethylamino)ethylamino] onto epoxy resin/silica coated substrates²⁶. Grafting all the silane coupling agents significantly improved mechanical properties of the epoxy resin, but using the middle chain length aminosilane, N-(2-aminoethyl)-3-aminopropyltrimethoxysilane, reported better improved thermo-mechanical properties²⁶.

Recent studies have shown that cells of the peripheral nervous system are mechanosensitive²⁷. Rosso *et al.* reported significantly higher Schwann cell attachment and neurite outgrowth from DRGs on stiffer substrates (20KPa) compared to softer substrates (1 and 10 KPa)²⁸ and Kayal *et al.* reported that

NG108-15 cell neurite outgrowth directionality could be controlled by substrate stiffness²⁷. However, it is difficult to compare our results with those of previously reported studies due to the magnitude in size of the DMT moduli reported for the clean glass, SC and LC modified surfaces, as well as differences in substrates modified. Future work will investigate these findings further.

All surfaces supported NG108-15 neuronal cell adhesion and viability. However, significantly higher numbers of live cells were observed adhering to LC modified surfaces compared to SC surfaces, and plain glass, suggesting LC aminosilane preferentially support NG108-15 neuronal cell viability. This agrees with the study by Buttiglione *et al.* whereby the addition of amine groups to PET surfaces, using plasma polymerisation, promoted SY5Y cell adhesion, increasing the surface charge of the substrate and increasing cellular adhesion via electrostatic attraction²⁹. Albumin, present in cell culture medium, has a higher affinity to both hydrophobic and rough surfaces which would explain the increased number of live cells attached to the LC modified surfaces³⁰.

This study has shown that the LC aminosilane preferentially supports NG108-15 neuronal cell differentiation consistently across an exposed surface area, compared to the SC modified and plain glass coverslips. NG108-15 neuronal cells were chosen for this study as they have been used for *in vitro* experiments in many peripheral nerve regeneration publications and are indicative of primary neuron responses³¹. NG108-15 neuronal cells extended significantly higher numbers of neurite-like processes per cell body, as well as significantly longer neurites when cultured on the LC modified surfaces in comparison to cells grown on SC aminosilanes or plain glass. Similar results were observed in Hopper *et al.* in which the addition of amine functionalised nano-diamond promoted NG108-15 cell

differentiation confirmed by an increase in NG108-15 neuronal cell bearing neurites and increase in average neurite length ³². Lizarraga-Valderrama *et al.* also reported that rougher surface topographies induced NG108-15 cell differentiation³³. The addition of LC aminosilane to glass substrates significantly increased average NG108-15 neuronal cell neurite outgrowth lengths and maximum neurite length. In addition to increasing surface roughness, the LC aminosilane could be providing chemical, and physical guidance cues, increasing neurite length. Chemical and physical guidance cues increase cell attachment, proliferation and differentiation, increasing neurite length of neurites outgrown from both NG108 neuronal cells and DRG explants ¹.

Amine modified surfaces supported Schwann cell attachment and cell viability. This was also observed in the study by Li *et al.* who reported that increasing the amount SC aminosilane used for modifying chitosan scaffolds increased primary Schwann cell attachment and proliferation ¹¹. Schwann cells cultured on all surfaces stained positively for GFAP, P75NGFR and S100 β antigens and Schwann cells cultured on LC modified glass exhibited and maintained a typical elongated phenotype, whereas cells cultured on the SC and plain glass surfaces exhibited a polygonal shape ¹⁸. This was quantified by calculating the aspect ratio of Schwann cells cultured on all surfaces, and was significantly higher on the LC surfaces compared to the aspect ratio of Schwann cells cultured on the plain and short chain modified glass. This observation was also reported by Hopper *et al.* in which typical elongated Schwann cells were observed on amine functionalised nano-diamond surfaces, and polygonal shaped Schwann cells observed on acrylic acid coated surfaces ³².

Surface modification of glass, using LC aminosilanization, has also been shown to preferentially support primary neuronal cell and Schwann cell attachment, and primary neuronal cell differentiation. Compared to plain glass, both SC and LC aminosilanes supported neuronal cell differentiation, identified by a significant increase in the average number of neurites per cell. However, the average neurite lengths of neurites extending from primary neurons were significantly longer when cultured on LC aminosilanes, compare to neurons grown on SC aminosilanes or plain glass. Previous studies have reported that the use of amine chemical reactive groups has been shown to increase neuronal cell differentiation^{32,34}. Naka *et al.* reported that patterned self assembling monolayers (SAMs), with amino terminal groups, promoted neurite outgrowth of embryonic chick DRG neurons and PC12 cells compared to SAMs with methyl and carboxyl groups³³. Ren *et al.* also reported that NH₂ modified glass surfaces induced differentiation of neural stem cells, compared to control groups³⁴.

Both LC and SC aminosilanes supported primary neuronal cell differentiation, identified by a significant increase in the average number of neurites sprouting from each neuron. This effect was not observed using NG108-15 cells. Although it is reported that NG108-15 cells can be indicative of primary neuron responses, data gathered is not always comparable to the *in vivo* response³⁶. This study opted to use dissociated DRGs as a primary cell model, to reduce the amount of animal usage (in line with the 3Rs) and obtain results indicative of the *in vivo* response¹². It was observed that primary Schwann cells were always in close proximity to neurite outgrowth which is important for nerve regeneration studies to observe neuronal cell-glial cell connections due to the role that Schwann cells have in nerve repair *in vivo*¹⁸. This study supports the value of more relevant cell sources, such as the

dissociated DRGs for neuronal and Schwann cell studies, highlighting differences between primary cell versus immortal cell lines for investigation of novel biomaterials in peripheral nerve repair.

In summary, we report on a surface deposition method with a LC aminosilane that increases hydrophobicity, surface roughness. This has the effect of supporting cell differentiation as determined by NG108-15 neuronal cells, and primary neurons cultured from dissociated DRGs. Both the SC and LC aminosilanes have been extensively characterised in our previous work and modification of glass substrates for neuronal cell differentiation was comparable to previous studies¹⁰. This is the first study to show that neuronal cell differentiation varies according to the length of the silane chain used. It also highlights the potential of silane modification as a scalable, cost effective approach, compared to using expensive ECM proteins, to functionalise existing biomaterials, used for neurosurgical scaffolds, with amine group surface modification for enhancing neuronal cell differentiation and supporting neuronal and Schwann cell viability.

ACKNOWLEDGEMENTS

We are grateful to Dr Nicola Green for experimental advice and assistance with confocal microscopy at the University of Sheffield (U.K.) Kroto Research Institute Confocal Imaging Facility.

ADDITIONAL INFORMATION

The authors do not have any competing financial interests associated with this work.

Conflict of Interest : None

Data Availability Statement: The data that support the findings of this study are openly available in figshare at <http://doi.org/10.15131/shef.data.13298195>, reference number 13298195.

REFERENCES

1. Bell, J.H. & Haycock, J.W. Next generation nerve guides: materials, fabrication, growth factors, and cell delivery. *Tissue Eng Part B Rev* 2012;18:116-128.
2. Behbehani, M., Glen, A., Taylor, C.S., Schuhmacher, A., Claeysens, F. & Haycock, J.W. Pre-clinical evaluation of advanced nerve guide conduits using a novel 3D in vitro testing model. *Inter J. of Bioprinting* 2018;4.
3. Daly, W., Yao, L., Zeugolis, D., Windebank, A. & Pandit, A. A biomaterials approach to peripheral nerve regeneration: bridging the peripheral nerve gap and enhancing functional recovery. *J R Soc Interface* 2012;9:202-221.
4. Chua, P.K., Chena, J.Y., Wang, L.P. & Huang, N. Plasma-surface modification of biomaterials. *Materials Science and Engineering R* 2002;36:143–206.
5. Curran, J.M., Chen, R. & Hunt, J.A. Controlling the phenotype and function of mesenchymal stem cells in vitro by adhesion to silane-modified clean glass surfaces. *Biomaterials* 2005;26:7057-7067.
6. Buttiglione, M., Vitiello, F., Sardella, E., Petrone, L., Nardulli, M., Favia, P., d'Agostino, R. & Gristina, R. Behaviour of SH-SY5Y neuroblastoma cell line grown in different media and on different chemically modified substrates. *Biomaterials* 2007;28:2932-2945.
7. Ni, H.C., Lin, Z.Y., Hsu, S.H. & Chiu, I.M. The use of air plasma in surface modification of peripheral nerve conduits. *Acta Biomater* 2010;6:2066-2076.

8. Ratner, B.D. Plasma deposition for biomedical applications: a brief review. *J Biomater Sci Polym Ed* 1992;4:3-11.
9. Fawcett, S.A., Curran, J.M., Chen, R., Rhodes, N.P., Murphy, M.F., Wilson, P., Ranganath, L., Dillon, J.P., Gallagher, J.A. & Hunt, J.A. Defining the Properties of an Array of -NH₂-Modified Substrates for the Induction of a Mature Osteoblast/Osteocyte Phenotype from a Primary Human Osteoblast Population Using Controlled Nanotopography and Surface Chemistry. *Calcif Tissue Int* 2017;100:95-106.
10. Chen, R., Hunt, J.A., Fawcett, S., D'sa, R., Akhtar, R. & Curran, J.M. The optimization and production of stable homogeneous amine enriched surfaces with characterized nanotopographical properties for enhanced osteoinduction of mesenchymal stem cells. *J Biomed Mater Res Part A* 2018;106A:1862-1877.
11. Li, G., Zhang, L., Wang, C., Zhao, X., Zhu, C., Zheng, Y., Wang, Y., Zhao, Y. & Yang, Y. Effect of silanization on chitosan porous scaffolds for peripheral nerve regeneration. *Carbohydrate Polymers* 2014;101:718-726.
12. Daud, M.F., Pawar, K.C., Claeysens, F., Ryan, A.J. & Haycock, J.W. An aligned 3D neuronal-glial co-culture model for peripheral nerve studies. *Biomaterials* 2012;33:5901-5913.
13. Kaewkhaw, R., Scutt, A.M. & Haycock, J.W. Integrated culture and purification of rat Schwann cells from freshly isolated adult tissue. *Nat Protoc* 2012;7:1996-2004.
14. de Luca, A.C., Faroni, A. & Reid, A.J. 2015 Dorsal Root Ganglia Neurons and Differentiated Adipose-derived Stem Cells: An In Vitro Co-culture Model to Study Peripheral Nerve Regeneration. *Journal of Visualized Experiments* 2015;52543.
15. Schneider, C.A., Rasband, W.S. & Eliceiri, K.W. NIH Image to ImageJ: 25 years of image analysis. *Nature Methods* 2012;9:671.

16. Usaj, M., Torkar, D., Kanduser, M. & Miklavcic, D. Cell counting tool parameters optimization approach for electroporation efficiency determination of attached cells in phase contrast images. *Journal of Microscopy* 2010;241:303-314.
17. Popko, J., Fernandes, A. & Lanier, L.M. Automated Analysis of NeuronJ Tracing Data. *Cytometry Part A : the journal of the International Society for Analytical Cytology* 2009;75:371-376.
18. Kaewkhaw, R., Scutt, A.M. & Haycock, J.W. Anatomical site influences the differentiation of adipose-derived stem cells for Schwann-cell phenotype and function. *Glia* 2011;59:734-749.
19. Zheng J, Kontoveros D, Lin F, Hua G, Reneker DH, Becker ML, Willits RK. Enhanced Schwann cell attachment and alignment using one-pot "dual click" GRGDS and YIGSR derivatized nanofibers. *Biomacromolecules* 2015;12;16(1):357-63.
20. T, C.S, Cost Effective Optimised Synthetic Surface Modification Strategies for Enhanced Control of Neuronal Cell Differentiation and Supporting Neuronal and Schwann cell Viability, 2020, 10.15131/shef.data.13298195
21. Lee, J.Y. & Schmidt, C.E. Amine-functionalized polypyrrole: Inherently cell adhesive conducting polymer. *J Biomed Mater Res Part A* 2015;103:2126-2132.
22. Crespin M, Moreau N, Masereel B, Feron O, Gallez B, Vander Borght T, Michiels C, Lucas S. Surface properties and cell adhesion onto allylamine-plasma and amine-plasma coated glass coverslips. *J Mater Sci Mater Med* 2011;22(3):671-82.
23. Love, J. C., Estroff, L. A., Kriebel, J. K., Nuzzo, R. G. & Whitesides, G. M. Self-Assembled Monolayers of Thiolates on Metals as a Form of Nanotechnology. *Chemical Reviews* 2005;105:1103-1170.

24. Anselme, K., Ploux, L. & Ponche, A. Cell/Material Interfaces: Influence of Surface Chemistry and Surface Topography on Cell Adhesion. *Journal of Adhesion Science and Technology* 2010;24:831-852.
25. Khan, R. A., Parsons, A. J., Jones, I. A., Walker, G. S. & Rudd, C. D. Effectiveness of 3-Aminopropyl-Triethoxy-Silane as a Coupling Agent for Phosphate Glass Fiber-Reinforced Poly(caprolactone)-based Composites for Fracture Fixation Devices. *Journal of Thermoplastic Composite Materials* 2011;24:517-534.
26. Tang, Y., Tang, C., Hu, D. & Gui, Y. Effect of Aminosilane Coupling Agents with Different Chain Lengths on Thermo-Mechanical Properties of Cross-Linked Epoxy Resin. *Nanomaterials (Basel, Switzerland)* 8, 951, doi:10.3390/nano8110951 (2018).
27. Kayal, C., Moeendarbary, E., Shipley, R.J. & Phillips, J.B. Mechanical Response of Neural Cells to Physiologically Relevant Stiffness Gradients. *Advanced Healthcare Materials* 2019;1901036.
28. Rosso, G., Liashkovich, I., Young, P., Röhr, D. & Shahin, V. Schwann cells and neurite outgrowth from embryonic dorsal root ganglions are highly mechanosensitive. *Nanomedicine: Nanotechnology, Biology and Medicine* 2017;13:493-501.
29. Metwalli, E., Haines, D., Becker, O., Conzone, S. & Pantano, C.G. Surface characterizations of mono-, di-, and tri-aminosilane treated glass substrates. *J Colloid Interface Sci* 2006;298:825-831.
30. Lukasiewicz, B., Basnett, P., Nigmatullin, R., Matharu, R., Knowles, J.C. & Roy, I. Binary polyhydroxyalkanoate systems for soft tissue engineering. *Acta Biomaterialia* 2018;71:225-234.

31. Armstrong, S.J., Wiberg, M., Terenghi, G. & Kingham, P.J. ECM molecules mediate both Schwann cell proliferation and activation to enhance neurite outgrowth. *Tissue Eng* 2007;13:2863-2870.
32. Hopper, A.P., Dugan, J.M., Gill, A.A., Fox, O.J., May, P.W., Haycock, J.W. & Claeysens, F. Amine functionalized nanodiamond promotes cellular adhesion, proliferation and neurite outgrowth. *Biomed Mater* 2014;9:045009.
33. Lizarraga-Valderrama, L.R., Nigmatullin, R., Taylor, C., Haycock, J.W., Claeysens, F., Knowles, J.C. and Roy, I. (2015), Nerve tissue engineering using blends of poly(3-hydroxyalkanoates) for peripheral nerve regeneration. *Eng. Life Sci* 2015;612-621.
34. Ren, Y.-J., Zhang, H., Huang, H., Wang, X.-M., Zhou, Z.-Y., Cui, F.-Z. & An, Y.-H. In vitro behavior of neural stem cells in response to different chemical functional groups. *Biomaterials* 2009;30:1036-1044.
35. Naka, Y., Eda, A., Takei, H. & Shimizu, N. Neurite outgrowths of neurons on patterned self-assembled monolayers. *Journal of Bioscience and Bioengineering* 2002;94:434-439.
36. Rayner, M.L.D., Laranjeira, S., Evans, R.E., Shipley, R.J., Healy, J. & Phillips, J.B. Developing an In Vitro Model to Screen Drugs for Nerve Regeneration. *Anat Rec* 2018;301:1628-1637.

FIGURE LEGENDS

FIGURE 1 - Dynamic water contact angle of glass, short chain (SC) and long chain (LC) aminosilane modified surfaces. Water contact angle significantly increased with addition of the aminosilanes compared to the plain glass control (mean \pm SD, n = 4 independent experiments; ***p < 0.001 and ****p < 0.0001 compared to plain glass).

FIGURE 2 - AFM analysis with scan size 1.4 μm x 1.4 μm : (A) Plain glass control; (B) SC aminosilane modified glass; (C) LC aminosilane modified glass; (D) elastic modulus of aminosilane-modified glass substrates (mean \pm SD, n=3; *p<0.05 and **p<0.01).

FIGURE 3 - Confocal micrographs illustrating NG108-15 neuronal cell viability cultured on: A) fibronectin control; B) Plain glass; C) SC aminosilane; D) LC aminosilane; and E) tissue culture plastic control. Scale bar = 100 μm . Cells labelled with syto 9 (green= live cells) and propidium iodide (red= dead cells). F) Number of live cells versus dead cells per sample (mean \pm SD, n=3 independent experiments; P< 0.05, **p<0.01, ***p<0.001 and ****p<0.0001) and G) live cell analysis expressed as percentage (mean \pm SD, n=3 independent experiments; P< 0.05).

FIGURE 4 - Confocal micrographs of NG108-15 neuronal cells immunolabelled for β III-tubulin and DAPI on: A) fibronectin control; B) Plain glass; C) SC aminosilane; D) LC aminosilane; and E) tissue culture plastic control. Scale bar = 100 μm . Confocal images were quantified to determine: F) The percentage of neurite bearing neuronal cells after 6 days in culture (mean \pm SD, n=3; p<0.05); G) the average number of neurites expressed per neuron (mean \pm SD, n=3; *p<0.05 and **p<0.01) and H) average neurite length per condition after 6 days in culture (mean \pm SD, n=3; *p<0.05, **p<0.01 and ***p<0.001). I) Maximum neurite length on all substrates.

FIGURE 5 - Confocal micrographs showing live/dead analysis of primary rat Schwann cells on: A) fibronectin control; B) Plain glass; C) SC aminosilane; D) LC aminosilane; and E) tissue culture plastic control. Scale bar = 100 μm . F) Number of live cells versus dead cells per sample and G) live cell analysis expressed as a percentage (mean \pm SD, n=3 independent experiments).

FIGURE 6 - Confocal micrographs of primary rat Schwann cells immunolabelled for S100 β (green), GFAP (red) and P75NGFR (yellow) after 6 days of culture on fibronectin controls, plain glass, SC and LC aminosilanes, and tissue culture plastic. Schwann cells were immunolabelled to confirm Schwann cell phenotype. P)

Average Schwann cell length; Q) aspect ratio (length/width) to identify Schwann cell phenotype (mean \pm SD, n=3; *p<0.05).

FIGURE 7 - Confocal micrographs of primary neurons and primary Schwann cells dissociated from dorsal root ganglion bodies and immunolabelled against β -III tubulin (red) and S100 β (green), and cell nuclei (DAPI; blue). Cells were cultured on: A) fibronectin control; B) Plain glass; C) SC aminosilane; D) LC aminosilane; and E) tissue culture plastic control. Scale bar = 100 μ m. F) Average numbers of neurites per neuron after 7 days in culture (mean \pm SD, n=3 *p<0.05 versus plain glass). G) Average neurite length (mean \pm SD, n=3, *p<0.05, **p<0.01, and ***p<0.001, versus LC aminosilane, #p<0.05 versus tissue culture plastic). H) Maximum neurite length on all substrates.

TABLE LEGEND

TABLE 1 – X-ray photoelectron spectroscopy characterization of glass surfaces after aminosilane modification. XPS elemental composition is shown as percentage of carbon, silicon, oxygen and nitrogen for glass control, short chain and long chain aminosilane-modified surfaces (mean \pm SD, n=4).